

## Rates for Color Shifted Microlensing Events

Ari Buchalter<sup>\*1</sup>, Marc Kamionkowski<sup>†2</sup>, and R. Michael Rich<sup>\*3</sup>

<sup>\*</sup>Department of Astronomy, Columbia University, New York, NY 10027

<sup>†</sup>Department of Physics, Columbia University, New York, NY 10027

### ABSTRACT

If the objects responsible for gravitational microlensing of Galactic-bulge stars are faint dwarfs, then blended light from the lens will distort the shape of the microlensing light curve and shift the color of the observed star during the microlensing event. In most cases, the resolution in current microlensing surveys is not accurate enough to observe this color-shift effect. However, such signatures could conceivably be detected with frequent followup observations of microlensing events in progress, providing the photometric errors are small enough. We calculate the expected rates for microlensing events where the shape distortions will be observable by such followup observations, assuming that the lenses are ordinary low-mass main-sequence stars in a rapidly rotating bar and in the disk. We adopt Galactic models consistent with observed microlensing timescale distributions, and consider separately the cases of self-lensing of the bulge, lensing of the bulge by the disk, and self-lensing of the disk, further differentiating between events where the source is a giant or a main-sequence star. We study the dependence of the rates for color-shifted microlensing events on the frequency of followup observations and on the precision of the photometry for a variety of waveband pairings. We find that for hourly observations in  $B$  and  $K$  with typical photometric errors of 0.01 mag, 28% of the events where a main-sequence bulge star is lensed, and 7% of the events where the source is a bulge giant, will give rise to a measurable color shift at the 95% confidence level. For observations in  $V$  and  $I$ , the fractions become 18% and 5%, respectively,

---

<sup>1</sup>ari@parsifal.phys.columbia.edu

<sup>2</sup>kamion@phys.columbia.edu

<sup>3</sup>rmr@cuphys.phys.columbia.edu

but may be increased to 40% and 13% by improved photometric accuracy and increased sampling frequency. Unlike standard achromatic lensing events, color-shifted events provide information on the lens mass, distance, and velocity. We outline how these parameters can be obtained, giving examples of typical errors which may arise in the calculation, and briefly discuss other applications of such light-curve measurements. We show that color-shifted events can be individually and/or statistically distinguished from events where the source is blended with a binary companion. In particular, the observed fraction of color-shifted events as a function of event timescale will test whether the color shift is caused by a lens which is a low-mass main-sequence star, or by a blended star.

*Subject headings:* Galaxy: general – Galaxy: structure — gravitational lensing

## 1. INTRODUCTION

The MACHO (Alcock et al. 1993, Alcock et al. 1995a), EROS (Aubourg et al. 1993), OGLE (Udalski et al. 1994a), and DUO (Alard et al. 1995) gravitational-microlensing surveys have yielded a wealth of interesting but puzzling results. Although the rate of microlensing of stars in the LMC appears to be too small for the lenses to account for the dark matter in the Galactic halo needed to support the Galactic rotation curve, the nature and location of the 6 MACHO lenses observed to date toward the LMC remain a mystery. Are they in a “maximal disk,” the halo, or perhaps in the LMC itself? Even more intriguing are the results of surveys of the Galactic bulge: the MACHO and OGLE groups have to date observed 85 and 12 lensing events, respectively, toward the bulge. The optical depth to microlensing toward the bulge appears to be 2-3 times higher than expected from lensing by low-mass stars in simple Galactic models. One possibility is that this enhancement is due to a hitherto undiscovered population of compact dark objects which suggests the existence of more mass in the disk than previously believed (Alcock et al. 1994, Gould 1994a). Another explanation is that the larger optical depth observed is due to structure, such as a bar, in the bulge (Kiraga & Paczyński 1994, hereafter KP; Zhao, Spergel, & Rich 1995, hereafter ZSR). Several lines of evidence seem to point to the latter possibility (Binney et al. 1991; Blitz & Spergel 1991; Whitelock & Catchpole 1992; Stanek et al. 1994; Dwek et al. 1995). In this case, the lenses would mostly be low-mass, but otherwise ordinary, stars in the bulge itself. Thus, gravitational microlensing is proving to be a primary tool in the understanding

of Galactic structure and in the study of stellar populations in the bulge and inner Galactic disk.

The optical depth to microlensing, the fraction of source stars undergoing microlensing at any given time, can be measured from the observed timescales (i.e., the event durations) and the frequency with which events occur, to give an approximation to the integrated mass in lenses along the line of sight. However, the timescale

$$t_0 = \frac{R_e}{v}; \quad R_e = \left( \frac{4GM_l D_{ol} D_{ls}}{c^2 D_{os}} \right)^{1/2}, \quad (1)$$

(the time the source star remains within the Einstein ring of the lens), where  $R_e$  is the Einstein radius, depends on the distances from the observer to both the source star and the lens,  $D_{os}$  and  $D_{ol}$ , the transverse speed  $v$  of the lens relative to the source-star line of sight, and the mass  $M_l$  of the lens (and  $D_{ls} \equiv D_{os} - D_{ol}$ ). Although the distances to the source stars in the LMC, and to a lesser extent in the bulge, are known to reasonable accuracy, the mass, speed, and distance of any given lens cannot be disentangled in any given event.

Several techniques for breaking the degeneracy in  $t_0$  have been proposed. Measurement of the amplification of limb brightening in giant source stars during a microlensing event could determine  $R_e/D_{ol}$  and  $v$  (Loeb & Sasselov 1995). The combination,  $v/D_{ol}$ , can be measured photometrically (Gould 1994b; Nemiroff & Wickramasinghe 1994) and spectroscopically (Maoz & Gould 1994). Measurement of microlensing parallaxes from a single satellite in heliocentric orbit could determine the “reduced” transverse speed and Einstein radius,  $(D_{os}/D_{ds})v$  and  $(D_{os}/D_{ds})R_e$ , respectively (Gould 1995a; Han & Gould 1995a). For the rare events with timescales comparable to a year, measurement of parallax from the ground can already be used to measure the reduced velocity, and such parallax shifts may be observable in a larger fraction of events with frequent and accurate followup observations (Buchalter & Kamionkowski 1995, in preparation). All of these techniques provide more information than that provided by just the timescale, although they still leave a two-fold degeneracy. (The degeneracy could be broken completely by a second parallax satellite.) Realistically, however, some of these ideas are effective only in a small fraction of events, and others will require several years to come to fruition.

Recent calculations of microlensing towards the bulge indicate that Galactic models having a mass function with 25% or more of the mass in the form of brown dwarfs are inconsistent with the current MACHO and OGLE data; the best-fit models have a number-averaged mean mass of  $0.3 M_\odot$  (ZSR; Zhao, Rich, & Spergel 1995, hereafter ZRS). If the lenses are indeed low-mass main-sequence stars, then another possibility exists for removing the degeneracy (Kamionkowski 1995). In that case, both the source star and lens fall within a single seeing disk and the light from the two becomes blended. However,

during the microlensing event, only the light from the source star is amplified. Stars generally have different colors, so during the event, the color of the two blended stars should change. Furthermore, the contribution of unlensed light from the lens will distort the shape of the standard microlensing light curve, even if there is no color difference. Accurate measurement of the light curves of color-shifted events (CSEs) can be used to obtain the brightness of the lens in two or more wavebands in which case the mass, distance, and transverse speed of the lens could be determined through spectroscopic parallax.

This color shift is unlikely to be dramatic enough to be observed by any of the existing surveys in all but a small fraction of events; the frequency with which the light curves are currently sampled is too small, and the photometric errors are too large. For existing data, color-shift analysis can only be used to constrain the lens mass as a function of distance (Kamionkowski 1995; Kamionkowski & Buchalter 1995; Alcock et al. 1995b). However, both the OGLE and MACHO collaborations have now developed an early-warning alert system which can signal a potential microlensing event in progress shortly after the light curve begins to rise (Stubbs et al. 1994; Udalski et al. 1994b). Therefore, it is conceivable that a program of followup observations of microlensing light curves in progress with frequent (e.g., hourly) measurements and small photometric errors could be used to measure the light curve with sufficient accuracy to pick out color shifts and shape distortions in a significant fraction of the events. In fact, such a followup program is already being considered with the primary purpose of detecting planets around the lenses (Tytler et al. 1996, in preparation). Planetary masses would give rise to smaller typical timescales (on the order of 2 to 50 hours) and thus produce narrow spikes on the lensing light curve which likely go undetected in current observations. These spikes could be resolved by dedicated telescopes performing rapid sampling of events in progress, with low photometric errors. The same survey would thus be ideal for the detection of color-shifted distortions.

In this paper, we evaluate the fraction of microlensing events toward the Galactic bulge which should have an observable shape distortion in such a followup program. We calculate the fractions that will arise if the lenses are all in the bulge and if the lenses are all in the disk. We consider surveys which focus only on source stars which are giants, and those in which the source stars are main-sequence stars. To do so, we use several realistic models for the distribution of lenses, with a timescale distribution which matches roughly that for the events observed so far. A Monte Carlo technique is then used to simulate events and generate shape-distorted microlensing light curves for each. It is then determined for each event whether the shape-distorted light curve can be distinguished at the 95% confidence level from a standard achromatic microlensing light curve. The calculation is performed for several viable values of the sampling frequency and for several values for photometric accuracies that are realistically attainable. The final results are displayed as a function of

sampling frequency for several different levels of photometric error.

Our results indicate that dedicated telescopes sampling events in progress at an hourly rate in  $B$  and  $K$  should observe a color shift planetary for roughly 30% of the events where a main-sequence bulge star is lensed (by either a disk or bulge star) given photometric errors of 0.01 mag. For the lensing of a bulge giant, the expected fraction drops to 7%. For rarer events where a disk source is lensed by a foreground disk star, the calculated rate of color shifting is 51% for dwarf sources and 8% for giants. We find comparable results for observations in  $V$  and  $I$ , yielding values typically 0.6 to 0.7 times those for  $B$  and  $K$ . The expected fraction of CSEs increases significantly as the photometric errors and sampling intervals are reduced; for data sampled every fifteen minutes in  $V$  and  $I$  with 0.005 mag errors, 40% of the events with bulge main-sequence sources and 13% of those with bulge clump-giant sources are expected to be color shifted. Events with this characteristic distortion to the microlensing light curve, including those where a mass is discovered, can be studied to directly infer the locations, masses, and transverse speeds of the lenses to within relatively small errors. Furthermore, light curves distorted by a luminous lens may be distinguished by various techniques from those where the source is merely blended with another star along the line of sight. We emphasize that the color-shifting effect must be observed by the intensive monitoring surveys if the lenses are low-mass dwarfs, and would thus provide direct evidence that normal stars are responsible for microlensing towards the bulge. In addition, color-shift analysis can be applied immediately to all events, so that information about the mass, velocity, and spatial distributions of the lensing population will become instantly accessible in many cases, without the need for long-term followup observations.

The plan of the paper is as follows: In Section 2, we review the characteristics of the shape distortions to the light curves. In Section 3, we outline the model used for our calculation, including the bulge and disk models employed, and the relations used to connect brightnesses with stellar masses. In Section 4, we calculate the timescale distribution for these models and compare with the currently observed distributions. Section 5 discusses the criteria used to determine whether a given event can be distinguished from a standard microlensing light curve with sufficient statistical significance. In Section 6, we consider what may be learned from existing data and present the results of our calculations of the expected fractions of CSEs. Section 7 addresses how well light-curve analysis in such experiments will be able to constrain the lens mass, distance, and speed. In Section 8, we discuss methods of distinguishing color-shifted events from ordinary blended events, and in Section 9 we make some concluding remarks.

## 2. COLOR-SHIFTED MICROLENSING EVENTS

Consider first ordinary achromatic microlensing by a nonluminous lens. If the distance of the lens from the source-star line of sight is  $R_e u$ , where

$$R_e = \left[ \frac{4G\mathcal{M}_l D_{ol}(D_{os} - D_{ol})}{c^2 D_{os}} \right]^{1/2} = 3.2 \text{ a.u.} \left[ \frac{\mathcal{M}_l}{\mathcal{M}_\odot} \frac{D_{os}}{8 \text{ kpc}} \frac{x'}{0.8} \frac{1-x'}{0.2} \right]^{1/2} \quad (2)$$

is the Einstein radius of the lens and  $x' = D_{ol}/D_{os}$ , then the amplification of the source star as a function of time  $t$  is

$$A[u(t)] = \frac{u^2 + 2}{u(u^2 + 4)^{1/2}}; \quad u(t) = \left[ \left( \frac{t - t_{\max}}{t_0} \right)^2 + u_{\min}^2 \right]^{1/2}, \quad (3)$$

where  $u$  is the impact parameter in units of the Einstein radius,  $t_0 = R_e/v$  is the event timescale,  $v$  is the transverse speed of the lens relative to the source-star line of sight, and  $t_{\max}$  is the time at which peak amplification,  $A_{\max} = A(u_{\min})$ , occurs.

A microlensing event is detected when the amplification exceeds  $A_T$  which corresponds to a dimensionless lens–line-of-sight distance of  $u_T$  (e.g.,  $A_T = 1.34$  for  $u_T = 1$ ). A standard achromatic event is described by three parameters:  $u_{\min}$  (or equivalently,  $A_{\max}$ ), the timescale  $t_0$ , and the time  $t_{\max}$ . The event duration  $t_e$  is the time that the amplification is above threshold, and it is also the time the lens remains within a distance  $u_T R_e$  from the line of sight; it is related to the timescale  $t_0$ . The system parameters (the distances to and masses of both stars and the transverse speed) cannot be determined uniquely in any given event. These quantities can in principle be disentangled in a statistical manner if a number of events are observed, and only with some assumptions about the mass, spatial, and speed distributions of the lenses. Microlensing is a gravitational effect, so the amplification is the same in all wavelengths. Therefore, if the lens is too faint to be observed, the event will be achromatic.

If the lens is itself an ordinary (although perhaps low-mass) main-sequence star, then it will emit light of its own. Therefore, let us now consider the effect of unlensed light from the lens on the microlensing light curve. The brightness of a star of luminosity  $L$  at a distance  $d$  is  $\ell = L/d^2$ . The source star with brightness  $\ell_s$  is lensed by a star with brightness  $\ell_l$ . The light observed is a combination of the light from both stars, and the colors of the two stars will generally be different (Griest & Hu 1992; Gould & Loeb 1992; Udalski et al. 1994c; Kamionkowski 1995). When the lens passes within the microlensing tube, the source star will be amplified, and the relative brightnesses will change. Consequently, the color will change, and achromaticity is lost. To properly describe the event, we must consider the

brightness in each waveband separately. If the amplification of the background star is  $A$ , then the brightness in waveband  $\lambda$  is  $\ell_\lambda = \ell_{l\lambda} + A\ell_{s\lambda}$ , where  $\ell_{l\lambda} = L_{l\lambda}/d_l^2$  is the brightness of the lens star in  $\lambda$ ,  $L_{l\lambda}$  is the luminosity of the star in  $\lambda$ , and similarly for the source star. The baseline brightnesses are obtained by setting  $A = 1$ .

Although  $A$  is the amplification of the source star, the observed light in this case comes from both stars, so the *observed* amplification, which we denote by  $\mathcal{A}$ , is different from the microlensing amplification  $A$ . Although the amplification of the background star is indeed achromatic, the observed amplification will depend on wavelength, and in waveband  $\lambda$  it is

$$\mathcal{A}_\lambda(t) = \frac{\ell_{l\lambda} + A(t)\ell_{s\lambda}}{\ell_{l\lambda} + \ell_{s\lambda}} = (1 - r_\lambda) + A(t)r_\lambda, \quad (4)$$

where  $r_\lambda = \ell_{s\lambda}/(\ell_{s\lambda} + \ell_{l\lambda})$  is the luminosity offset ratio (note  $r_\lambda = 1$  for a completely dark lens). Suppose, for example, light curves are measured in two bands,  $\alpha$  and  $\beta$ . If  $\ell_l \gtrsim \ell_s$  (in both bands), then the baseline color observed will be  $\ell_{l\alpha}/\ell_{l\beta}$  (the color of the lens), but in a lensing event with amplification  $A \gg 1$ , the observed color will be  $\ell_{s\alpha}/\ell_{s\beta}$  (the color of the background star). In general, a color-shifted event will be registered when the *observed* amplification is greater than threshold,  $\mathcal{A} > A_T$ . This depends on the band, so strictly speaking, the exact time at which an event is registered (or whether it is registered at all) may depend on the waveband. If events are triggered by the light curve in  $\lambda$ , they will be registered when the microlensing amplification is  $A \geq A_{\text{thresh}} = [A_T - (1 - r_\lambda)]/r_\lambda$ , or only when the dimensionless lens–line-of-sight distance is  $u \leq u_{\text{thresh}} = u(A_{\text{thresh}})$ . The duration of an event,  $t_e = 2t_0[u_{\text{thresh}}^2 - u_{\text{min}}^2]^{1/2}$ , depends on the transverse speed, the mass of the lens, the distances to both stars through  $t_0$ , the brightnesses of both stars through the  $r$  dependence of  $u_{\text{thresh}}$ , and on the impact parameter. In all cases, the duration of such color-shifted events should be shorter than the duration of achromatic events (Kamionkowski 1995).

Figure 1 illustrates an example of a microlensing light curve distorted by the color-shift effect. Note that the different light curves have the *same* values of  $t_0$  and  $u_{\text{min}}$ , and differ only in  $r_\lambda$ . In addition to the shift in amplification, the contribution of the unlensed light changes the *shape* of the microlensing light curve in any given band as well. In Figure 2, we plot a simulated color-shifted light curve with  $t_0 = 30$  days,  $u_{\text{min}} = 0.1$  and  $r_\lambda = 0.5$ . This curve has a peak amplification of 5.52 and a FWHM of 12.1 days. We also plot an achromatic light curve (i.e., only 3 parameters) with the same peak height and FWHM (both curves are assumed to have  $t_{\text{max}} = 0$ ). The two curves and the residuals show that they have different shapes, and that the effect of color shifting is observable along the *entire* light curve. It is important to note that if a color-shifted lensing event is fit for only the three achromatic parameters  $t_0$ ,  $t_{\text{max}}$ , and  $A_{\text{max}}$ , the inferred values can be substantially

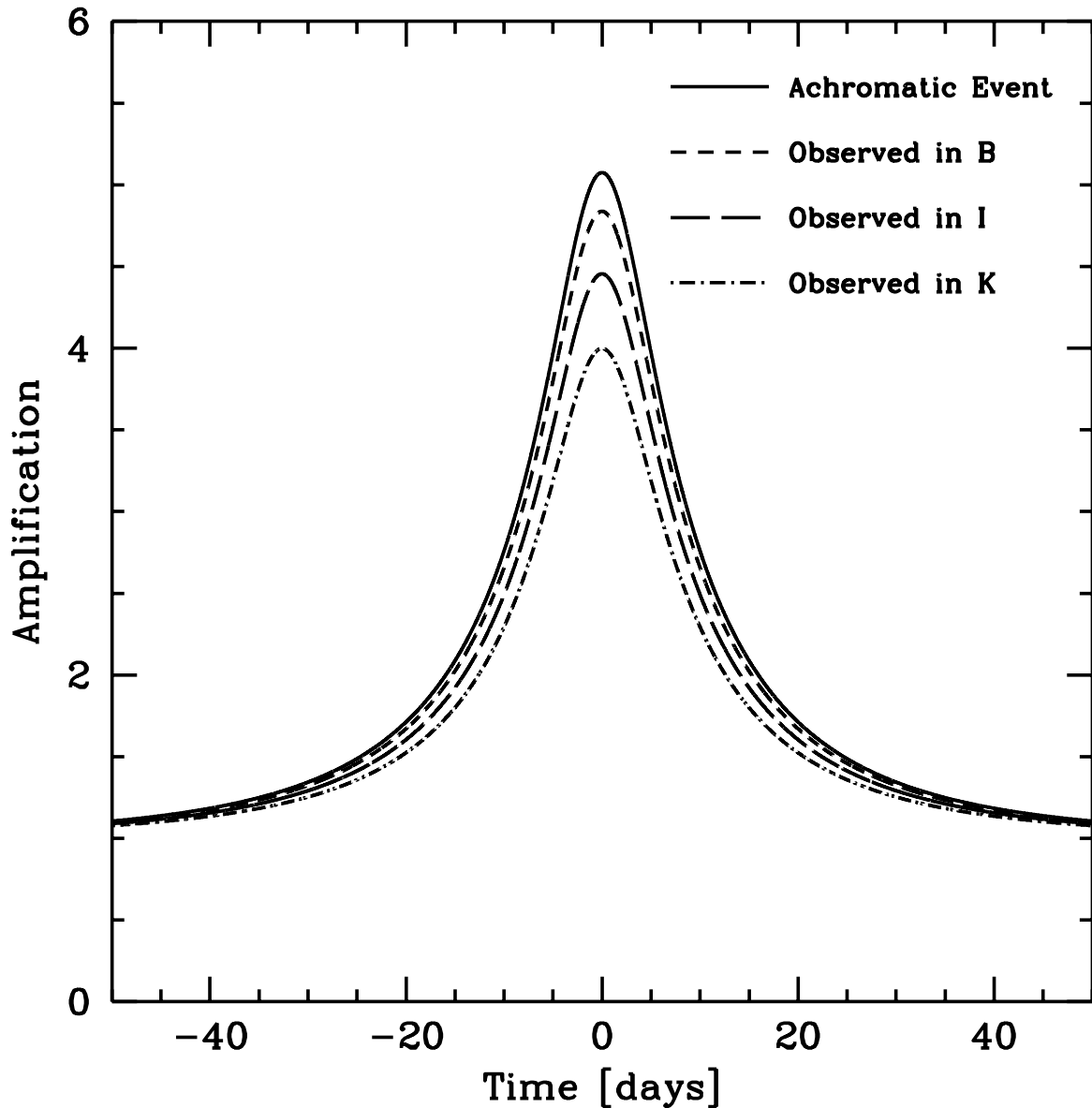


Fig. 1.— Microlensing light curve for a  $0.6M_{\odot}$  object at 4 kpc lensing a  $1M_{\odot}$  main-sequence star at 8 kpc. The solid curve represents the standard achromatic amplification (i.e., for a “dark” lens) in any waveband. The dashed curves represent the same event observed in different wavebands if we assume the lens is a main-sequence star. The light curves were all generated with the same  $t_0$ ,  $t_{\max}$ , and  $u_{\min}$ , but with differing values of  $r_{\lambda}$  in the different bands as given by the assumed stellar mass-luminosity relations (see below).

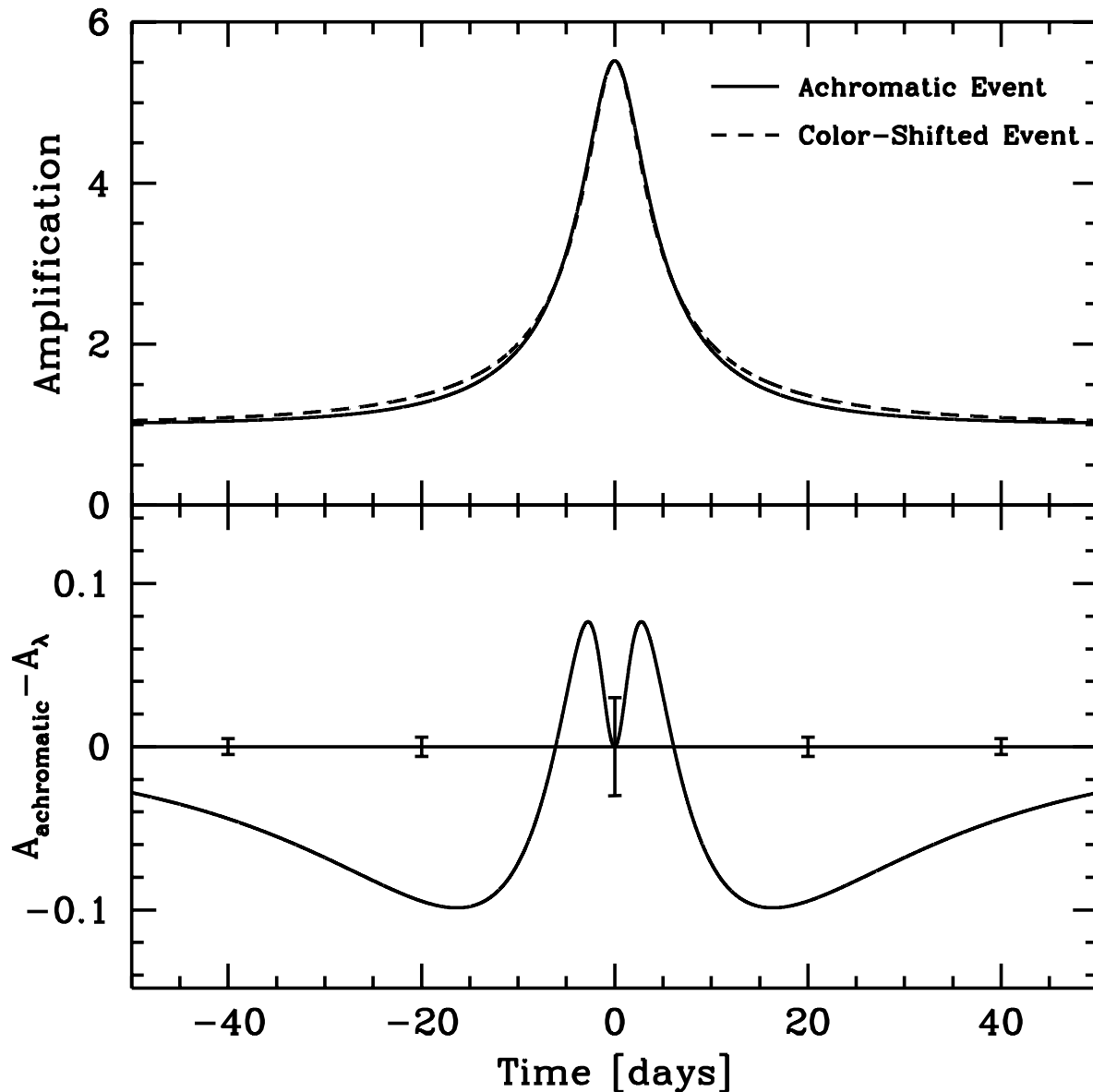


Fig. 2.— The upper panel shows a color-shifted light curve (dashed line) with parameters  $t_0 = 30$  days,  $u_{\min} = 0.1$ , and  $r_{\lambda} = 0.5$ , and an achromatic light curve (solid line) with identical peak height and FWHM. The achromatic curve has  $t_0 = 18.12$  days and  $u_{\min} = 0.18$ . The lower panel shows the residuals in  $A_{\text{achromatic}} - A_{\lambda}$ , along with typical expected errors for the proposed planetary surveys.

different from their true values. In this case the best achromatic fit to the color-shifted curve yields the incorrect values of  $t_0 = 18.12$  days and  $u_{\min} = 0.18$ , values which are in error by roughly 40% and 80%, respectively. The “true” achromatic curve corresponding to the event would have a larger peak height and FWHM, as in Figure 1.

If both the source and lens are main-sequence stars, then the source is usually brighter than the lens in most of the events that will be detected (Kamionkowski 1995). Moreover, if the sources are giants, the source will almost always be much brighter than the lens. As a result, color shifting and shape distortions to the light curves will usually be small. Therefore, we will heretofore neglect the small effect of unlensed light on the threshold amplification and event duration.

### 3. GALACTIC MODEL

Gravitational microlensing has rapidly become an important tool for understanding Galactic structure. Yet despite the large event rate observed toward the Galactic bulge, the basic characteristics of the lens population are unknown due to the simultaneous dependence of the relevant parameters  $M_l$ ,  $D_{ol}$ , and  $v$  on the fitted parameter  $t_0$ . Observation of shape distortions to microlensing light curves may help break the degeneracy. In particular, such distortions can potentially be observed using high-precision, intensive monitoring. Therefore, we construct a model to calculate the expected fraction of events along the line of sight to Baade’s Window ( $\ell = -1^\circ$ ,  $b = 4^\circ$ ) in which a color-shift distortion will arise. We consider separately three scenarios of self-lensing of the Galactic bulge, lensing of the bulge by the disk, and self-lensing of the disk. Here we describe the bulge and disk models, as well as the mass-luminosity and color-color relations employed in the calculation. The halo is not expected to make any significant contribution to the optical depth toward the bulge.

#### 3.1. Bar Model

For the bar, we use the model of Zhao (1995), a numerically-constructed, self-consistent model of a rapidly-rotating bar. The density profile matches the Dwek et al. (1995) fit to the COBE image of the Galaxy, and the velocity dispersions match those inferred from measured proper motions (Spaenhauer, Jones, & Whitford 1992) and radial velocities (Rich 1988, 1990). (See Zhao 1995 and ZRS for a more detailed discussion). The bar model

consists of 2,308 stars generated from a Monte Carlo of Zhao’s phase-space distribution, each with a distance along the line of sight to Baade’s Window, and proper motions  $v_\ell$  and  $v_b$ .<sup>4</sup>

Our analysis of CSEs depends on the stellar mass functions. Though the luminosity function of the bulge is not well constrained, several groups have used microlensing observations to fit the bulge mass function (MF). Both ZRS and Han & Gould (1995b), using data from 55 MACHO and OGLE events, find the best fitting MF to be a power law ( $dN/d\mathcal{M} \propto \mathcal{M}^{-p}$ ) with an index  $p$  between 2 and 2.5, and a lower mass cutoff near  $0.1 \mathcal{M}_\odot$ . Following KP, we adopt a logarithmic MF,  $dN/d\mathcal{M} \propto \mathcal{M}^{-2}$ , in the range  $0.1\mathcal{M}_\odot \leq \mathcal{M}_l \leq 1.2\mathcal{M}_\odot$ , which is consistent with the observed MACHO and OGLE timescale distributions (see ZRS Figure 2).

### 3.2. Disk Model

For the galactic disk, we adopt a double exponential profile with

$$\rho_d \propto \exp(-R/h_R) \exp(-z/h_z), \quad (5)$$

where  $\rho_d$  is the density of stars,  $R$  and  $z$  are Galactocentric radial and vertical coordinates and  $h_R = 3.5$  kpc and  $h_z = 350$  pc are the radial and vertical scale lengths. We assume the value  $\rho_{d,\odot} = 0.1\mathcal{M}_\odot\text{pc}^{-3}$  at a solar Galactocentric distance of 8 kpc. The color-magnitude diagram (CMD) of stars in bulge fields shows a deficit of foreground disk stars (Paczynski et al. 1994). Thus, following KP and ZRS, we truncate the disk beyond 5 kpc from the solar circle, leaving a central hole of radius 3 kpc. The corotation radius of the bar extends only to 3 kpc from the Galactic center, so the disk and bulge stars in our model can be distinguished by their distance alone. We assume a constant disk rotation speed of  $v_\phi = 220$  km s<sup>-1</sup> (Merrifield 1992). Lewis & Freeman (1989) measured the velocity dispersions of disk stars and found relations of the form  $\sigma_{R,\phi}(R) = \sigma_{R,\phi}(0) \exp[-R/2h_{R,\phi}]$  for the radial and azimuthal velocity dispersions, and it is assumed that  $\sigma_z(R) \propto \sigma_R(R)$ . Van der Kruit (1988) studied the vertical velocity dispersions in external spirals and found the additional relation  $\sigma_z(z) = \sigma_z(0) \exp[-z/h_z]$ , where  $\sigma_z$  increases by a factor of 1.3 at 500 pc above the midplane. We adopt this relation, together with slopes of

---

<sup>4</sup>We thank H. S. Zhao for providing this sample.

$d(\log\sigma_\phi)/dR = 0.064 \text{ km s}^{-1} \text{ kpc}^{-1}$  and  $d(\log\sigma_R)/dR = 0.051 \text{ km s}^{-1} \text{ kpc}^{-1}$  from Lewis & Freeman (1989). In this case,  $\sigma_{\phi,z}$  are both given by

$$\log\sigma_{\phi,z}(x) = \log\sigma_{\phi,z}(0) + 0.065x \quad (6)$$

where  $x$  is distance measured inward from the solar circle in kpc,  $\sigma_\phi(0) = 20 \text{ km s}^{-1}$ , and  $\sigma_z(0) = 17 \text{ km s}^{-1}$ . Azimuthal drift is typically of order 1/5 the dispersion along the line of sight (Merrifield 1992) and is neglected.

The main peak of the observed microlensing timescales can be accounted for by bulge self-lensing (ZRS), so unlike the case for the bulge, the data do not place strong constraints on the disk MF. If the assumed bulge MF is also adopted for the disk, the resulting duration distribution is consistent with MACHO and OGLE observations in the sense of fitting the main peak (see ZRS Figure 2). However, the present-day MF of the disk is believed to follow a power-law behavior which flattens out around sub-solar masses (Scalo 1986, Larson 1986). Scalo (1986) finds a flattening in the MF below  $1.0\mathcal{M}_\odot$  with a maximum near  $0.3\mathcal{M}_\odot$ , while HST observations by Gould, Bahcall, & Flynn (1995) find a maximum near  $0.5\mathcal{M}_\odot$ . Furthermore, the line of sight to Baade’s Window reaches a height of 350 pc above the plane at 5 kpc, so the most massive stars with typical  $\sigma_z = 10 \text{ km s}^{-1}$  and lifetimes  $< 10^8 \text{ yr}$  will generally not be seen along the line of sight (B3 stars, with a lifetime of  $2 \times 10^7 \text{ yr}$  can only be expected to reach a height of 200 pc). However, B5 stars, with a lifetime of  $2 \times 10^7 \text{ yr}$ , may typically reach 600 pc (Mihalas & Binney 1982), and A stars are observed by Rodgers & Harding (1989) at latitudes of  $b = 25^\circ$ . Thus, we will also consider the HST MF,  $\log\phi = 1.35 - 1.34 \log(\mathcal{M}/\mathcal{M}_\odot) - 1.85 [\log(\mathcal{M}/\mathcal{M}_\odot)]^2$  in the range from  $0.1\mathcal{M}_\odot \leq \mathcal{M}_l \leq 5.0\mathcal{M}_\odot$ , as well as a composite power-law MF with  $dN/d\mathcal{M} = 0$  for  $0.1\mathcal{M}_\odot \leq \mathcal{M}_l \leq 0.4\mathcal{M}_\odot$ ,  $dN/d\mathcal{M} \propto \mathcal{M}^{-1.25}$  for  $0.4\mathcal{M}_\odot \leq \mathcal{M}_l \leq 1.0\mathcal{M}_\odot$ ,  $dN/d\mathcal{M} \propto \mathcal{M}^{-2.3}$  for  $1.0\mathcal{M}_\odot \leq \mathcal{M}_l \leq 3.0\mathcal{M}_\odot$  and  $dN/d\mathcal{M} \propto \mathcal{M}^{-3.2}$  for  $3.0\mathcal{M}_\odot \leq \mathcal{M}_l \leq 5.0\mathcal{M}_\odot$  (Mihalas & Binney 1982). Presumably, any nearby disk lenses near or above our upper mass cutoff would be easily identifiable.

### 3.3. Mass-Luminosity and Color-Color Relations

Absolute  $V$  and  $K$  magnitudes for main-sequence stars in the range  $0.1\mathcal{M}_\odot \leq \mathcal{M}_l \leq 1.2\mathcal{M}_\odot$  (whether sources or lenses) were calculated using the mass-luminosity relations found by Henry & McCarthy (1993) for the lower main sequence. The CMD of stars in Baade’s Window indicates a main-sequence turnoff point near  $1 \mathcal{M}_\odot$  with a systematic brightening, at nearly constant color, of stars near the turnoff

that have undergone some post-main-sequence evolution (Vandenberg & Laskarides 1987). Thus, bulge stars more massive than  $0.9 \mathcal{M}_\odot$  were assumed to be semi-evolved and given an increase in magnitude between 0 (for  $0.9 \mathcal{M}_\odot$ ) and 1 (for  $1.2 \mathcal{M}_\odot$ ).  $B$  and  $V$  magnitudes for disk stars more massive than  $1.2 \mathcal{M}_\odot$  were obtained using a 10th order fit to mass-luminosity data from Allen (1973). Sources corresponding to clump giants were assumed to have absolute magnitudes of 0.335 and 1.43 in the  $I$  and  $V$  bands, respectively. All stellar magnitudes in other bands were obtained using polynomial color-color relations derived from accurate photometric data (Caldwell et al. 1993). The distribution of source magnitudes and colors obtained with this model resembles the OGLE data (Udalski et al. 1994a).

A simple model for reddening was adopted wherein the dust is confined to a narrow layer centered on the Galactic midplane. The extinction in each waveband,  $a_\lambda$ , is thus assumed to increase linearly with distance out to 2 kpc, beyond which the line of sight to Baade’s Window breaks free of the dust layer (Arp 1965), and all sources and lenses are assumed to suffer maximal extinction, according to the standard extinction curve given by Savage & Mathis (1979).

It remains to relate  $r_\lambda$  to the apparent luminosities and apparent magnitudes. Since

$$m_\lambda = -2.5 \log \ell_\lambda + \text{constant}, \quad (7)$$

where  $m_\lambda$  is the apparent magnitude in waveband  $\lambda$ , we can write  $r_\lambda$  as

$$r_\lambda = \frac{\ell_{s\lambda}}{\ell_{s\lambda} + \ell_{l\lambda}} = \left(1 + 10^{[(m_{s\lambda} + a_{s\lambda}) - (m_{l\lambda} + a_{l\lambda})]/2.5}\right)^{-1}. \quad (8)$$

#### 4. TIMESCALE DISTRIBUTION

The optical depth is defined to be the probability that any given star falls within the Einstein ring (of cross section  $\pi R_e^2$ ) of a lens. For a source at a distance  $D_{os}$ , the optical depth is

$$\tau(D_{os}) = \int_0^{D_{os}} dD_{ol} n_l(D_{ol}) \pi R_e^2, \quad (9)$$

where  $n_l(D_{ol})$  is the number of lenses per unit volume at a distance  $D_{ol}$  from the observer. Using  $R_e^2 = 4GM_d D/c^2$ , where  $D \equiv (D_{os} - D_{ol})D_{ol}/D_{os}$ , we find

$$\tau(D_{os}) = \frac{4\pi G}{c^2} \int dD_{ol} \rho_l(D_{ol}) D, \quad (10)$$

where  $\rho_l$  is the mass of lenses per unit volume along the line of sight. For a fixed lens mass density, the optical depth is independent of the mass.

The number of source stars undergoing microlensing (i.e., which fall behind the Einstein ring of a lens) at any given time is

$$N = \frac{4\pi G}{c^2} \int_0^\infty \tau(D_{os}) n_s(D_{os}) dD_{os}, \quad (11)$$

where  $n_s(D_{os})$  is the number of sources per unit length (in contrast to  $n_l$ , which is a number per unit volume) along the line of sight. So we may write

$$N = \frac{4\pi G}{c^2} \int_0^\infty dD_{os} n_s(D_{os}) \int_0^{D_{os}} dD_{ol} \int d\mathcal{M}_l \frac{d\rho_l}{d\mathcal{M}_l} \int dv f(v, D_{ol}, D_{os}). \quad (12)$$

Here, we have included the expression for  $\tau(D_{os})$ . Furthermore, we have included an integral over the mass distribution  $d\rho_l/d\mathcal{M}_l$  (where  $\mathcal{M}_l$  is the lens mass) of the lens mass density, and an integral over the velocity distribution function  $f(v, D_{ol}, D_{os})$ . The quantity  $v$  is the transverse speed of the lens through the microlensing tube, so the velocity distribution function will in general depend on the lens and source distances. If the mass function of lenses is independent of distance, then the distribution may be written

$$\frac{d\rho_l}{d\mathcal{M}_l} = \rho_l(D_{ol}) \frac{1}{\langle \mathcal{M}_l \rangle} \frac{d\mathcal{N}}{d\mathcal{M}_l} \quad (13)$$

where  $d\mathcal{N}/d\mathcal{M}_l$  is the lens lens mass function and  $\langle \mathcal{M}_l \rangle$  is the mean lens mass. The velocity and mass distribution functions are normalized such that

$$\int \mathcal{M}_l \frac{d\mathcal{N}}{d\mathcal{M}_l} d\mathcal{M}_l = \langle \mathcal{M}_l \rangle \quad \text{and} \quad \int f(v, D_{os}, D_{ol}) dv = 1. \quad (14)$$

Therefore, Eq. (12) can be written,

$$N = \frac{4\pi G}{c^2 \langle \mathcal{M}_l \rangle} \int_0^\infty dD_{os} n_s(D_{os}) \int_0^{D_{os}} dD_{ol} \rho_l(D_{ol}) \int dm m \frac{d\mathcal{N}}{dm} \int dv f(v, D_{ol}, D_{os}). \quad (15)$$

The total number of sources undergoing microlensing at any given time is independent of the lens-mass and velocity distributions, so the integrals in Eq. (15) evaluate trivially to unity. They are included for use in the next step.

The distribution of timescales  $t_0 = R_e/v$  for all events in progress at any given time is

$$\begin{aligned} \frac{dN}{dt_0} = & \frac{4\pi G}{c^2 \langle \mathcal{M}_l \rangle} \left[ \int_0^\infty dD_{os} n_s(D_{os}) \int_0^{D_{os}} dD_{ol} \rho_l(D_{ol}) D \right. \\ & \left. \int d\mathcal{M}_l \mathcal{M}_l \frac{d\mathcal{N}}{d\mathcal{M}_l} \int dv f(v, D_{ol}, D_{os}) \delta(t_0 - \sqrt{4G\mathcal{M}_l D}/(cv)) \right]. \quad (16) \end{aligned}$$

The frequency of events with time scales in the range  $t_0$  to  $t_0 + dt_0$  is

$$\frac{d\Gamma}{dt_0} dt_0 = \frac{2}{\pi t_0} \frac{dN}{dt_0} dt_0, \quad (17)$$

so<sup>5</sup>

$$\begin{aligned} \frac{d\Gamma}{dt_0} = & \frac{4G^{1/2}}{c \langle \mathcal{M}_l \rangle} \left[ \int_0^\infty dD_{os} n_s(D_{os}) \int_0^{D_{os}} dD_{ol} \rho_d(D_{ol}) D^{1/2} \right. \\ & \left. \int d\mathcal{M}_l \mathcal{M}_l^{1/2} \frac{d\mathcal{N}}{d\mathcal{M}_l} \int dv v f(v, D_{ol}, D_{os}) \delta(t_0 - \sqrt{4G\mathcal{M}_l D}/(cv)) \right]. \quad (18) \end{aligned}$$

Due to the presence of the  $\delta$  function in Eq. (16), the prefactor  $t_0^{-1}$  can be taken inside the integral and evaluated to  $t_0 = \sqrt{4G\mathcal{M}_l D}/(cv)$ . The expression for the total frequency  $\Gamma$  is obtained by removing the  $\delta$  function in this expression.

The total number of events which are observed to peak within any given observing period of duration  $\Delta t$  (assumed to be long compared with  $t_0$ ) is  $N_{\text{peak}} = \Gamma \Delta t$ , so the observed timescale distribution is

$$f(t_0) \propto \frac{d\Gamma}{dt_0} \epsilon(t_0). \quad (19)$$

where we have explicitly included the observation detection efficiency  $\epsilon(t_0)$ . Following ZSR, we adopt the function  $\epsilon(t_0) = 0.3 \exp[-(t_0/11 \text{ days})^{-0.7}]$  as a good interpolation of the values given in Udalski et al. (1994) for the OGLE data. The MACHO efficiencies are typically higher for a given event duration (Alcock et al. 1995b), but do not significantly alter our results for color shifting.

The MACHO and OGLE surveys, which sample events roughly daily with typical errors of roughly 0.05 mag, do not constrain the microlensing light curves sufficiently to pick out color shifting in most cases. Thus, the condition that events be achromatic should have little effect on the observed timescale distribution for events of short duration (i.e.,  $t_0 \leq 20$  days). However, longer-duration events, with better sampled light curves, are expected to yield a greater fraction of CSEs, particularly for the case of disk lensing (see Sections 7 and 8, and Figure 10). If the achromaticity condition is strong, it will then have the effect of systematically eliminating larger fractions of the longer events, so that the contribution of these events to the overall duration distribution would be suppressed relative to the “actual” distribution. This effect becomes more dramatic as the sampling interval and errors are reduced. If most of the lenses are in the form of main-sequence stars, this leads to

---

<sup>5</sup>We thank A. Gould for a discussion of the timescale distribution.

the danger that the resulting color shifts prevent the detection of those events for which the degeneracy in  $t_0$  can be broken entirely. However, the current MACHO collaboration cut on achromaticity is sufficiently weak that this is unlikely to be a problem (Griest 1995). In particular, we estimate that this effect is negligible for the case of bulge self-lensing, which accounts for most of the observed events, and is only expected to shift the disk lensing peaks by about 10% towards the shorter end.

The duration distributions for the disk and bulge models used are shown in Figure 3. The relative peak heights have not been normalized. ZRS fits the Zhao bar model to 55 MACHO and OGLE events and finds that the best-fit model, with a median lens mass of  $0.18\mathcal{M}_\odot$ , predicts 40 bar events with a mean duration of 16 days, and 14 disk events with a mean duration of 30 days. Our bar model, with a median lens mass of  $0.185\mathcal{M}_\odot$  is nearly identical to that of ZRS and fits the main peak of the observed MACHO and OGLE distributions (see ZRS, Figure 2).

The distributions for the various MF models differ considerably. ZRS finds that the logarithmic disk MF is consistent with current microlensing data, but this MF differs considerably from that of the solar neighborhood. The HST and composite power-law MFs, derived from observations of the disk, produce peak durations near 40 and 63 days respectively, due to events where disk stars lens bulge stars. These results are less consistent with the main peak of the MACHO and OGLE distribution. However, both Han and Gould (1995b, see their Figure 3) and ZRS find significant fractions of observed events with  $t_0 \geq 60$  days, including an apparent bump in the duration distribution near  $t_0 = 100$  days, which are not accounted for by their models. The longer events in particular seem to be systematically located closer to the Galactic plane than the rest of the events (Zhao, private communication; see Figure 1 of Bennett et al. 1995), which suggests a disk origin. Our disk models using the HST and power-law MFs predict significant contributions from disk-lensing-bulge events at long durations, particularly by the latter. Furthermore, both models predict broad peaks near 60 and 90 days, respectively, due to disk self-lensing. Mollerach & Roulet (1995) also predict a substantial number of long-term events arising from disk lensing. Therefore, we speculate that the excess of long-duration events arise from disk-bulge and disk-disk lensing, with the lower amplitudes simply corresponding to the smaller optical depth of the disk. In this scenario, the larger timescales would probably arise from massive lenses with low velocity dispersions, i.e., nearby bright stars, but no conspicuously bright lenses have been identified. It is likely, however, that color-shift analysis should help to constrain the nature of these long-term events.

Another explanation for the long-term events would be a distribution of sources *and* lenses associated with the so-called “young” disk, having mean velocity dispersions of 10 km

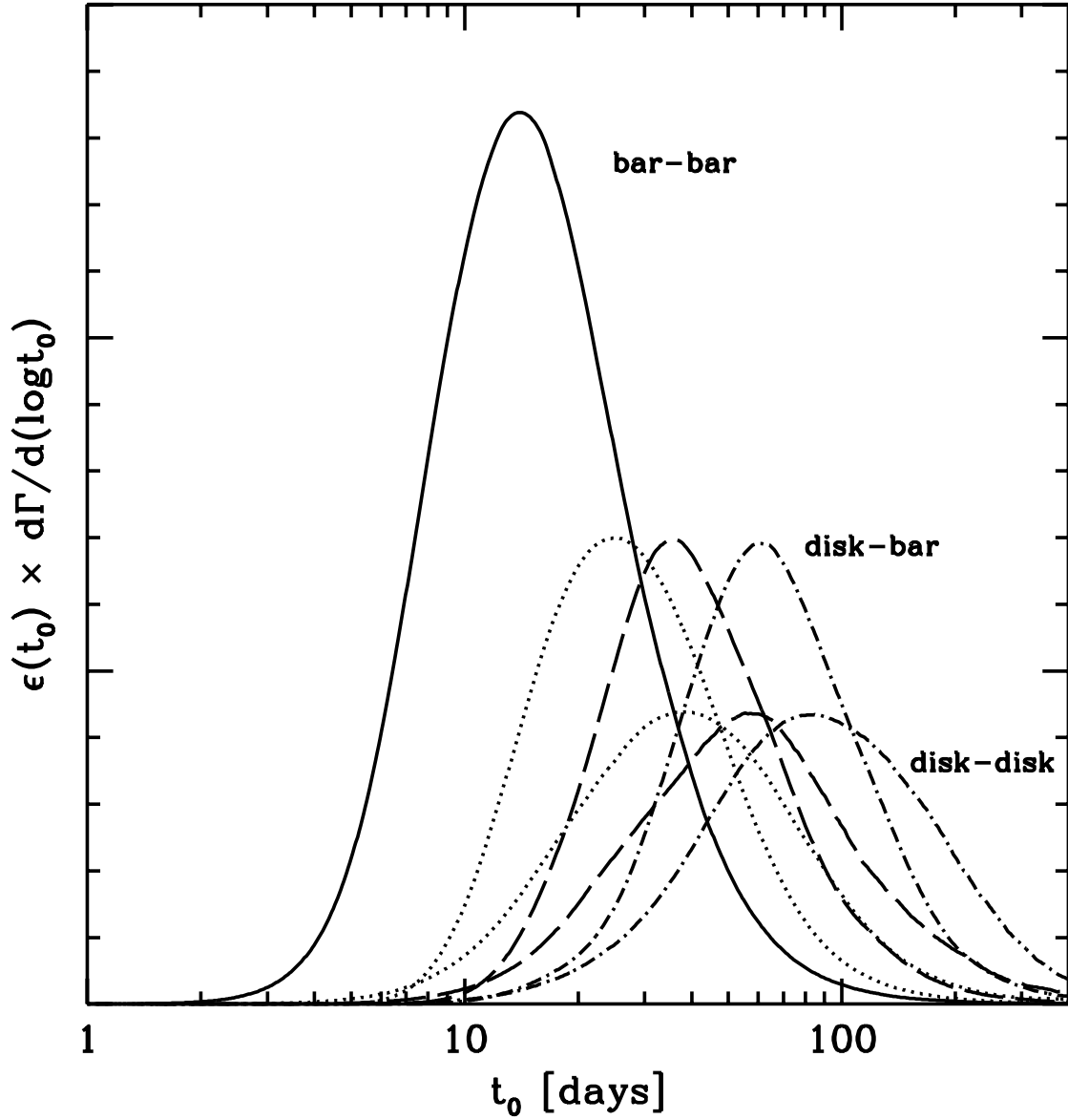


Fig. 3.— Predicted microlensing event duration distributions (non-normalized) for the bulge and disk models used. The main peak due to bulge self-lensing matches the peak of the observed MACHO and OGLE distributions. The dotted, dashed and dot-dashed curves represent the logarithmic, HST, and composite power-law disk MFs, respectively. We speculate that the disk lensing events may account for the few long-duration events observed.

$s^{-1}$  characteristic of the gas layer. A low-mass population (e.g., following the logarithmic disk MF) with these characteristics would also give rise to a broad disk self-lensing peak near  $t_0 = 100$  days (although this would require more mass in the young disk than usually assumed), while the higher-dispersion population would remain consistent with the main peak.<sup>6</sup> It is currently believed that the young disk accounts for 20% of the disk light (van der Kruit 1990). Han and Gould (1995b) point out that a similar result is obtained assuming the existence of a disk population of black holes, white dwarfs, and neutron stars which have low dispersion. Improved microlensing statistics will help to constrain better the MF of the lens population. In calculating the expected rates for CSEs, we conservatively adopt the logarithmic MF for the disk, noting that the low median lens mass in this model implies a lower limit on the color-shifting rate for disk events.

## 5. SENSITIVITY TO SIGNAL

Given the bar and disk models above, we wish to investigate the fraction of events that give rise to events which have observable shape distortions and/or color shifts.

As explained above, the amplification observed during a microlensing event in waveband  $\lambda$  is given by Eq. (4) where  $A(t)$  is the microlensing amplification in Eq. (2). If  $A_T$  is set, there are three parameters,  $t_{\max}$ ,  $A_{\max}$ , and  $t_0$ , which are needed to specify  $A(t)$ . There is then an additional parameter,  $r_\lambda$ , the luminosity offset ratio, needed to describe the light curve,  $\mathcal{A}_\lambda(t)$ . Therefore, color-shifted light curves in a number  $n$  of different wavebands are fit by  $3 + n$  parameters. (The baseline brightnesses in the  $n$  wavebands must also be fit; however, here we assume that the long-baseline observations of the source stars before and after the event will assure that the baselines brightnesses will be measured to great precision.)

We will consider frequently sampled followup observations of microlensing events and investigate the sensitivity of such a program to shape distortions in the microlensing light curves. We parameterize the various possible observing strategies first by the frequency of sampling, so measurements of the brightnesses in each waveband are obtained at times  $t_i$  separated by a time interval  $\Delta t$ . We also consider different photometric accuracies. Since the change in magnitude and the amplification are related by  $\Delta m = 2.5 \log A$ , a constant error in  $m$  translates to a constant percent error in  $A$ . Thus we will assume that any given

---

<sup>6</sup>We thank R. Olling for this suggestion.

measurement of the amplification has a gaussian distribution centered at the true value with a variance  $\sigma_l \simeq f\mathcal{A}(t_l)$  which is some fraction  $f$  of the amplification corresponding to the magnitude error.

To determine whether the shape distortion in a given event—specified by some source-star and lens masses and distances—will be observable, we first calculate the expected observed amplification  $\mathcal{A}(t)$ , and then ask whether light-curve measurements with a given sampling frequency and fractional error will produce a value of  $r_\lambda$  that is different from unity at the 95% confidence limit. If one of the unlensed-light parameters  $r_\lambda$  differs from unity with this statistical significance, then a shape distortion from unlensed light has been observed.

Suppose that the light curves are sampled  $N$  times and the error on each measurement  $i$  is gaussian distributed about the mean with a variance  $\sigma_i$ , as discussed above. Any given light curve  $\mathcal{A}(t, \mathbf{s})$  will depend on the set of parameters  $\mathbf{s} = \{A_{\max}, t_{\max}, t_0, r_\lambda\}$  (for  $\lambda = 1, \dots, n$ ). If the predicted parameters for a given event are  $\mathbf{s}_0$ , then the probability distribution for observing a light curve which is best fit by the parameters  $\mathbf{s}$  is (Gould 1995b; Jungman et al. 1995)

$$P(\mathbf{s}) \propto \exp \left[ -\frac{1}{2} (\mathbf{s} - \mathbf{s}_0) \cdot [\alpha] \cdot (\mathbf{s} - \mathbf{s}_0) \right], \quad (20)$$

where the curvature matrix  $[\alpha]$  is given approximately by

$$\alpha_{ij} = \sum_{l=1}^{nN} \frac{1}{\sigma_l^2} \left[ \frac{\partial \mathcal{A}(t_l, \mathbf{s}_0)}{\partial s_i} \frac{\partial \mathcal{A}(t_l, \mathbf{s}_0)}{\partial s_j} \right], \quad (21)$$

where the sum is over each measurement of the amplification in every waveband observed. The covariance matrix is given by  $[\mathcal{C}] = [\alpha]^{-1}$ . It is an estimate of the matrix of standard errors that could be obtained by a fit to data and is used to define the elliptical boundary of a desired confidence region. The projections of the ellipse define the corresponding confidence interval  $\delta \mathbf{s}$  on the parameters of interest. For our purposes, if the “true” value of the unlensed-light parameter is  $r_\lambda$ , the probability of observing a light curve which is best fit by a value  $r_\lambda^{\text{obs}}$  is a gaussian centered on  $r_\lambda$  with a variance  $\delta r_\lambda$  (68.3%), which corresponds to the  $1\sigma$  confidence level. As we cycle through each event, if  $\delta r_\lambda$  (95%)  $< (1 - r)$  for any  $\lambda$ , then the given event will have a shape distortion that can be distinguished with 95% confidence, and we accept this as a shape-distorted event. Otherwise, the event cannot be distinguished from a standard achromatic microlensing light curve. Our simulation included only those events in which the source star had an apparent magnitude of  $V < 21.0$ , and the event duration  $t_e$  satisfied  $2 \text{ days} \leq t_e \leq 1 \text{ year}$ . All included events were weighted by their frequency as given by Eq. (18) and summed to give an overall normalization. The

fraction of color-shifted events,  $F_{CSE}$ , is then defined as the ratio of the weighted sum of all color-shifted events to the overall normalization.

## 6. RESULTS

### 6.1. Accessible Masses

Before turning to our calculation of expected rates for CSEs, we determine, for a typical event, the values of  $\mathcal{M}_l$  (as a function of  $D_{ol}$ ) which will produce an observable color shift, considering separately the cases of main-sequence and clump-giant sources in the bulge. Given identical achromatic light curves in two wavebands  $\lambda_1$  and  $\lambda_2$ , each consisting of  $N$  points with normally distributed errors  $\sigma_1^{(i)}$  and  $\sigma_2^{(i)}$ , we can find the minimum values of  $r_{\lambda_1}$  and  $r_{\lambda_2}$  consistent with unity (i.e., achromaticity) at the 95% confidence level. In other words we look for the maximum possible  $\ell_{d\lambda}$  consistent with the assumption of achromaticity ( $\ell_{s\lambda}$  is assumed to be known). Together with an assumed mass-luminosity relationship, this places an upper limit on the lens mass as a function of distance, at the desired confidence level. This upper limit can be established from observations in a single waveband. However, multiple wavebands provide additional independent limits and thus tighter constraints. Figures 4 and 5 display upper limits on  $\mathcal{M}_l$  as function of  $D_{ol}$ , from observations in different wavebands, for typical events with main-sequence and giant sources at 8 kpc, respectively. We assume an event timescale of  $t_0 = 15$  days, near the peak of the bulge self-lensing duration distribution, and a minimum impact parameter of  $u_{\min} = 0.2$ . Any lens mass above the curves will give rise to a detectable color shift at the 95% confidence level, for the observational parameters listed in the Figure caption.

The results show that redder wavebands, where the lenses are assumed to emit most of their light, yield the strongest constraints on the lens mass all the way down to our lower cutoff of  $0.1\mathcal{M}_\odot$ . In particular, we find that for events with main-sequence sources, observed in  $K$  and either  $B$  or  $V$ , any lenses with  $\mathcal{M}_l > 0.18\mathcal{M}_\odot$  and all lenses in our model closer than 4 kpc in general, will give rise to a measurable color shift at the 95% confidence level. The results in the bluer wavebands, and for giant sources in general, are less dramatic, since the fractional contribution of the lens light will be smaller. The typical maximum achromatic lens masses in these cases are 0.3 to 0.6  $\mathcal{M}_\odot$  and 0.5 to 0.8  $\mathcal{M}_\odot$ , respectively. Of course, if the photometric errors are reduced, and/or the sampling frequency is increased, the constraints on the lens mass become stronger. The upper limits also decrease for larger event timescales.

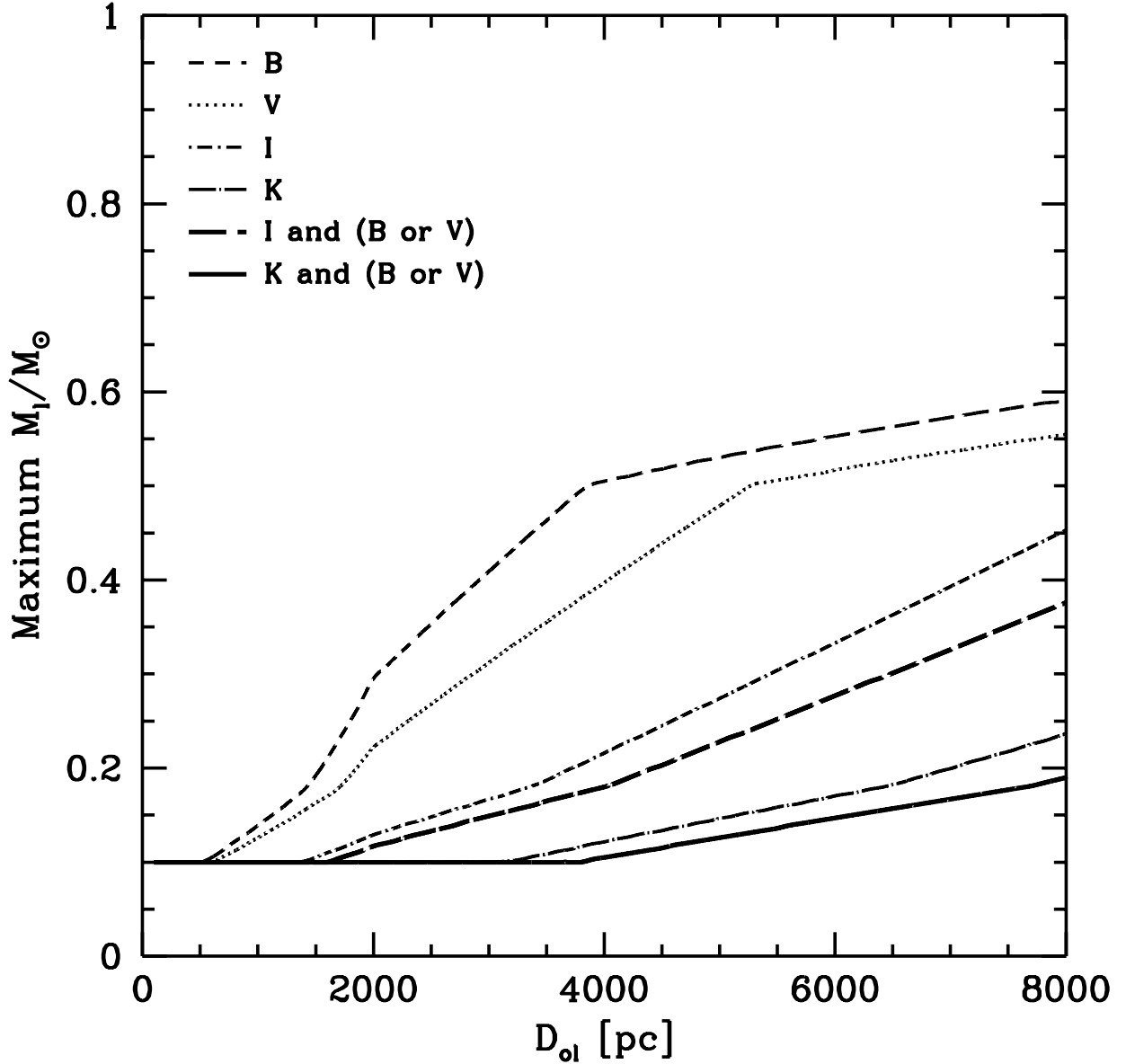


Fig. 4.— Upper limits on the lens mass,  $\mathcal{M}_l$ , as a function of observer-lens distance,  $D_{ol}$ , at the 95% confidence level for a model event with  $D_{os} = 8$  kpc,  $t_0 = 15$  days,  $u_{\min} = 0.2$  and simulated data with 0.01-mag normally distributed errors, taken hourly while  $A > A_T = 1.34$ . The source star is a  $1.0M_\odot$  main-sequence star. Note that the strongest constraints come from *I* and *K*, and in particular that for events observed in *K* and either *B* or *V*, all lenses toward the bulge with  $\mathcal{M}_l \geq 1.8M_\odot$  will give rise to a color shift. All results were obtained using the mass-luminosity and color-color relations stated above. The kinks are due to the tri-modal nature of the Henry & McCarthy (1993) mass-luminosity relationships.

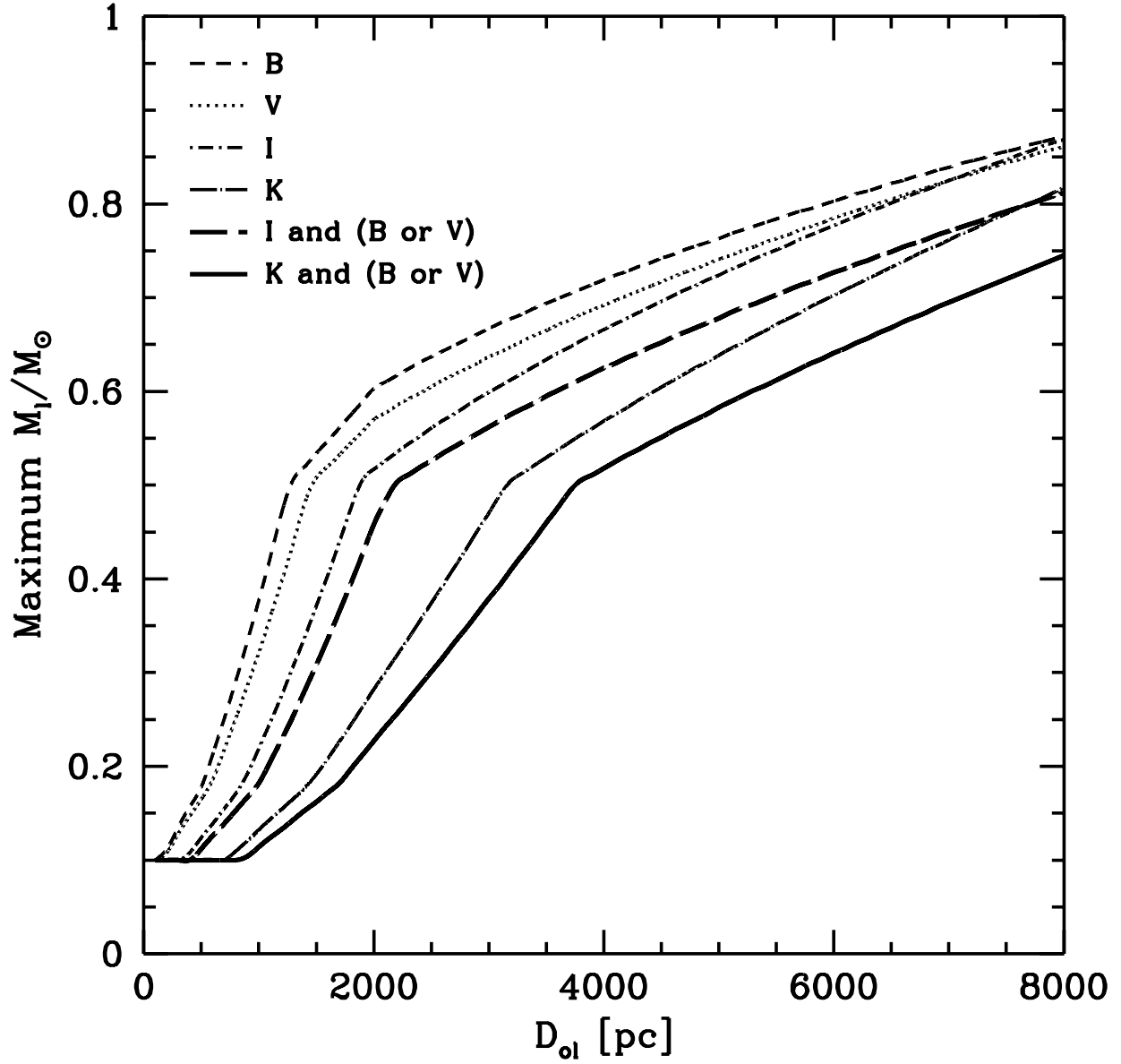


Fig. 5.— Same as Figure 4, with a clump-giant source at 8 kpc. The constraints are weaker due to the smaller fractional contribution of the faint lens to the amplification of the brighter source.

We further applied this analysis to the MACHO-collaboration parallax event (Kamionkowski & Buchalter 1995; Alcock et al. 1995b), since this event represents the most well-sampled existing microlensing light curve. To do so, we simulated the light curve, sampling frequency, and photometric errors of the observed event. Our results are shown in Figure 6, and agree with the results of Alcock et al. (1995b). The weaker constraints on the lens mass, as compared to Figure 5, suggest that surveys conducted with higher sampling frequency and greater photometric precision will significantly improve our knowledge of the lens MF.

## 6.2. Color-Shifted Fractions

Having illustrated what masses and distances will give observable distortions of the light curves, we now employ our Galactic model to calculate the overall expected fractions of color-shifted events (i.e., for all timescales), as functions of sampling frequency and photometric error. We distinguish between surveys focussed on source stars which are giants (denoted G) and those focussed on main-sequence sources (denoted MS). Despite smaller photometric errors, giants are expected to give rise to fewer CSEs, since the relative contribution of the faint main-sequence lens to the overall light profile will be small compared to the amplification of the bright giant star. We also consider separately the cases of bulge self-lensing (BB), disk stars lensing bulge sources (DB), and disk self-lensing (DD), giving rise to a total of six possible scenarios. Although the disk lensing events contribute less to the overall optical depth (particularly in the case of self-lensing of the disk), the transverse speed of disk lenses through the microlensing tube will be characteristically lower than that of bulge lenses, giving rise to longer-duration events. Such events will be more heavily sampled and thus more likely to yield a color shift. In all cases, the full geometrical depth of the bulge and/or disk is taken into account. We first consider observations made in  $B$  and  $K$ , denoted by  $(B,K)$ , since these bands are well-separated in wavelength and thus provide a large baseline for detecting color shifts. We also investigate the expected fractions for  $(V,I)$  to determine whether CCD photometry and infrared imaging are necessary for observing this effect. The logarithmic disk MF, which is consistent with the main timescale peak of the observed MACHO and OGLE events, is expected to give the fewest detectable color shifts for disk events. We examine this case and later compare with other MFs.

Figures 7 and 8 display the results of our Monte Carlo simulations, showing  $F_{CSE}$ , the fraction of events which are observably distorted, as a function of sampling interval, for events observed in  $(B,K)$  and  $(V,I)$ , respectively, for the various configurations. The solid,

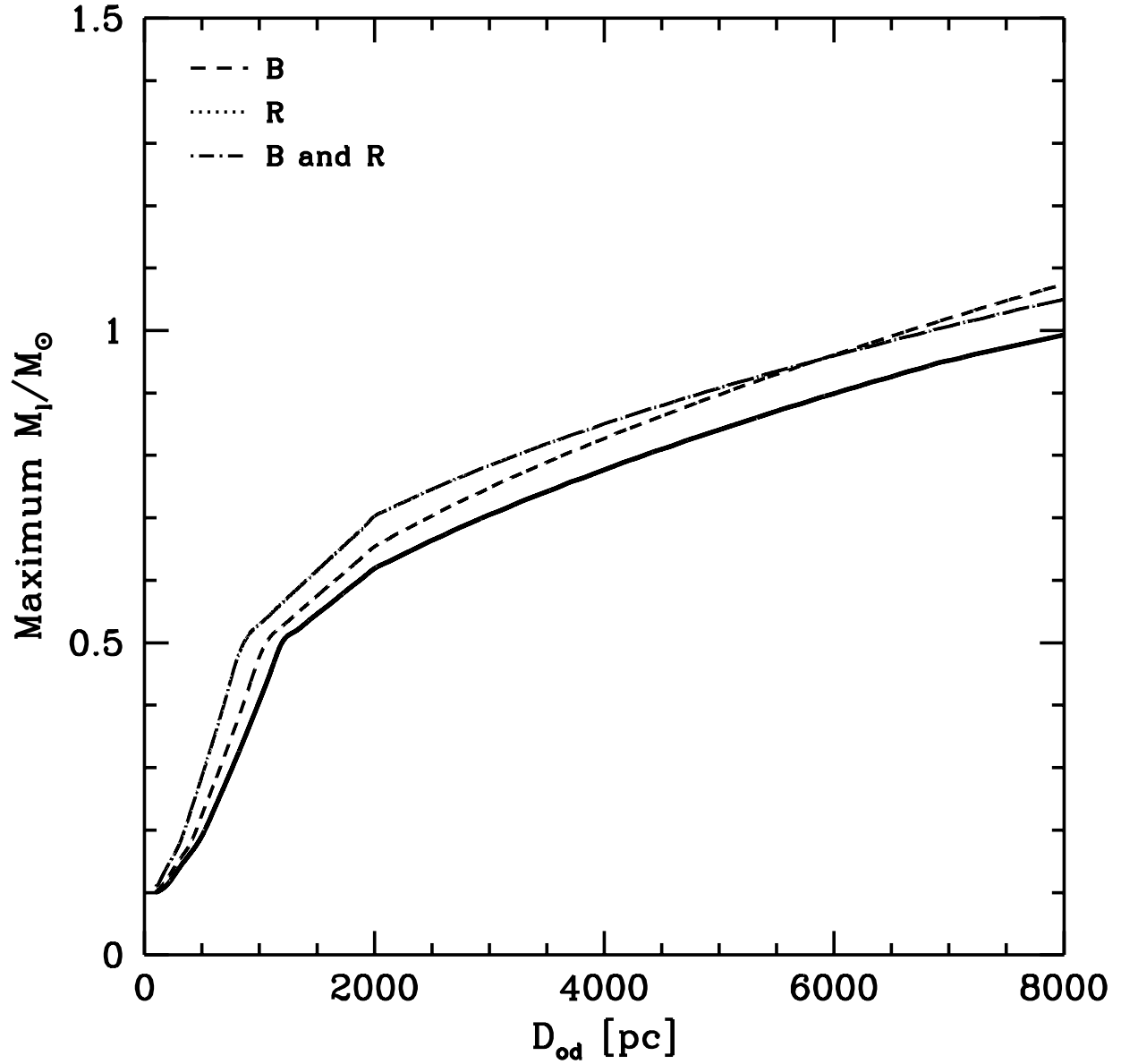


Fig. 6.— Upper limits on  $\mathcal{M}_l$  as a function of  $D_{ol}$  at the 95% confidence level for the MACHO-collaboration parallax event, with simulated parameters  $D_{os} = 8$  kpc,  $t_0 = 100$  days,  $u_{\min} = 0.1$  and “data” with 0.03-mag errors, taken every 24 hours while  $A > A_T = 1.34$ .

short-dashed, and long-dashed curves represent photometric errors of 0.05, 0.01 and 0.001 mag, respectively. The results verify that existing data on microlensing towards the bulge, with typical photometric errors of up to 0.05 mag and daily sampling rates at best, is not expected to be sensitive to these small distortions. Even for the most favorable lens-source configurations [namely DB(MS) and DD(MS)], current surveys, which use  $(V,R)$  or  $(V,I)$ , should only observe a color shift in fewer than 4% of the events; for the most likely scenario, BB(MS), the expectation is less than 2%. However, the Figures indicate significant increases in  $F_{CSE}$  for sampling intervals less than 5 hours, and particularly for intervals less than 1 hour. Furthermore,  $F_{CSE}$  increases dramatically as the errors are reduced. The intensive microlensing monitoring programs which have been proposed incorporate both of these improvements, and should reveal a much higher incidence of color shifting.

Figure 7 shows that for *all* cases of lens-source pairings at least a few percent of the events will be observably distorted, given frequent sampling and good photometry in  $B$  and  $K$ . For the most likely scenario of a bulge star lensing a bulge main-sequence star [BB(MS)], we find the expected fraction of color-shifted events is  $F_{CSE} = 0.25$ , given 0.01-mag photometric errors and an hourly sampling rate. In the more favorable case of a disk star lensing a main-sequence bulge star [DB(MS)], we find  $F_{CSE} = 0.43$  given the same observational parameters. Since the disk optical depth to microlensing is roughly 1/5 that of the bulge (ZSR), we estimate that 28% of the events where a main-sequence bulge star is lensed should yield a measurable color shift. For the case of a bulge giant being lensed, the relative contributions of  $F_{CSE} = 0.05$  from BB(G) and  $F_{CSE} = 0.14$  from DD(G) imply an overall expected color shifting rate of 7%. Moreover, if the light curve is sampled every 15 minutes, the expected fractions jump to 37% for bulge main-sequence sources and 10% for giants.

At first glance, it might be expected that the rare disk-on-disk events, with lower characteristic transverse speeds, would yield significantly higher fractions of color shifts due to the increased event duration  $t_0 = R_e/v$ . However, since more disk stars come into view of the solid angle toward the point where the disk is truncated ( $dN/dD_{ol} \propto D_{ol}^2$ ), the decrease in  $v$  is offset by a decrease in the typical lens-source separation [i.e. the factor  $D = (D_{os} - D_{ol})(D_{ol}/D_{os})$  in  $R_e$ ], unlike in the disk-lensing-bar case where the two model populations are spatially differentiated. Thus for hourly sampling and 0.01-mag errors,  $F_{CSE} = 0.51$  for DD(MS), slightly greater than the value for DB(MS), while DD(G) is expected to yield  $F_{CSE} = 0.08$ . For 15-minute sampling, these become 60% and 14%, respectively.

It is also of interest to examine the dependence of  $F_{CSE}$  on the choice of wavebands, to determine whether CCD photometry and infrared imaging are necessary to observe this

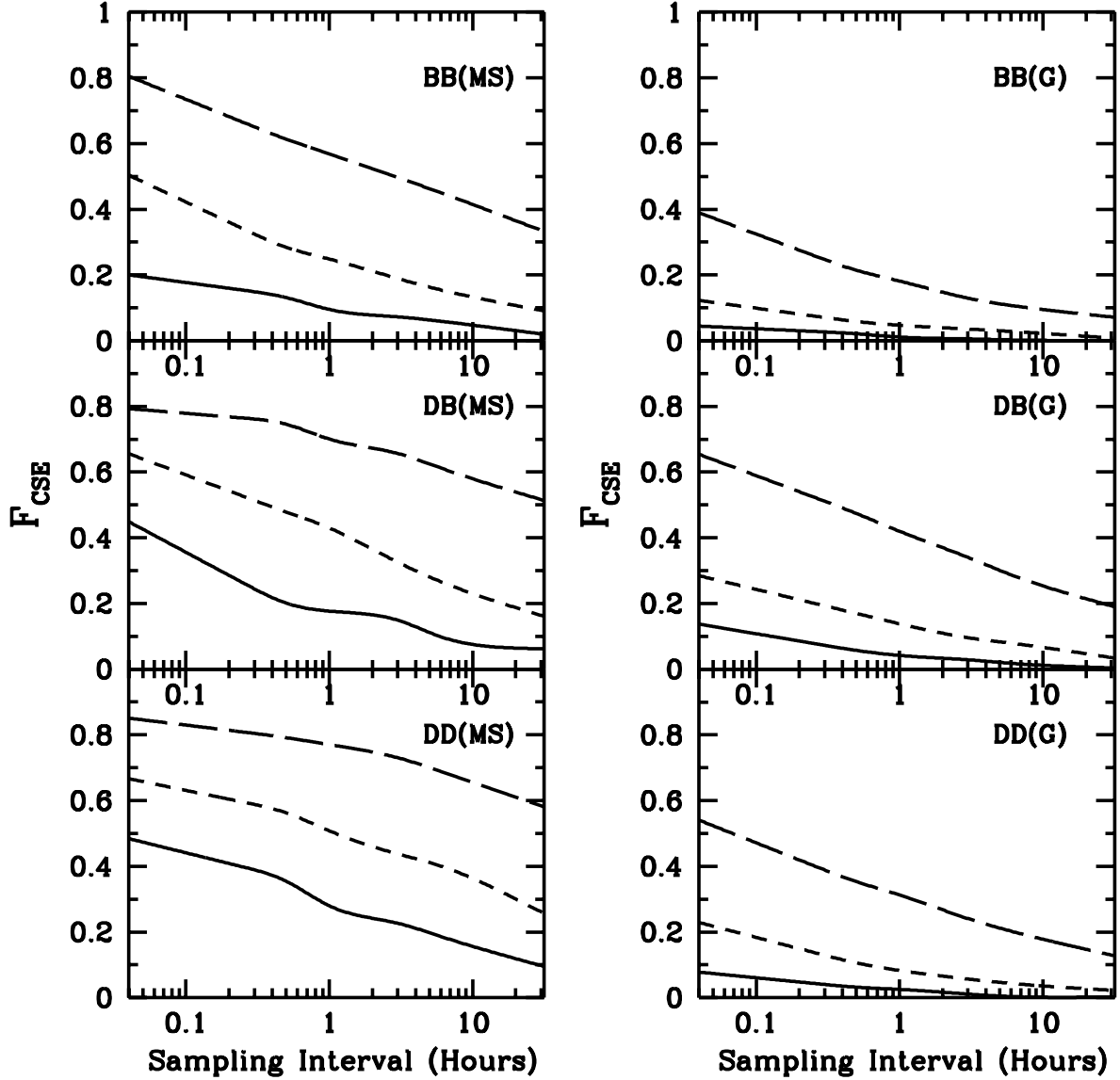


Fig. 7.— Expected fractions of CSEs as a function of sampling interval for events observed in  $B$  and  $K$ . The solid, short-dashed, and long-dashed lines correspond to photometric errors of 0.05, 0.01, and 0.001 mag, respectively. The various configurations are denoted by BB for bulge self-lensing, DB for disk-lensing-bulge events, and DD for disk self-lensing. MS indicates that the sources are main-sequence stars, while G indicates clump-giant sources.

effect. Figure 8 shows the results of our calculation done using  $(V,I)$ . We find that the expected rates remain significantly high, ranging from 0.6 to 0.7 times those for  $(B,K)$  in all cases. As mentioned above, the results for intermediate waveband pairings are determined primarily by the longest waveband used so that  $(V,K)$  and  $(B,I)$  yield virtually the same results as  $(B,K)$  and  $(V,I)$ , respectively. For all wavebands,  $F_{CSE}$  can be increased by improved statistics from multiple dedicated telescopes at different locations. For imaging in  $(V,I)$ , however, it is conceivable that high-precision photometry could potentially reduce errors to the millimagnitude regime, which is unlikely in the  $B$  and  $K$  bands. Together with a reduced sampling interval of 15 minutes, this improvement could increase the overall likelihood of observing color shifting of bulge sources to over 40% for main-sequence stars and 13% for giants, for events observed in  $(V,I)$ . For disk self-lensing the expected fractions can reach 60% for dwarf sources and 20% for giants.

We also note that if the stellar MF of the disk in the range between  $0.1M_{\odot}$  and  $1M_{\odot}$  is in fact flatter than the assumed logarithmic distribution, the increase in the median lens mass (and thus luminosity) would significantly increase the expected fraction of CSEs for cases where the lens is a disk star. In Figure 9, we compare  $F_{CSE}$  using the logarithmic, HST, and composite power-law MFs, for the case of disk stars lensing bulge main-sequence stars [DD(MS)], for simulated observations in  $V$  and  $I$  with 0.01-mag errors. The dramatic increase suggests that our calculations of  $F_{CSE}$  for disk events actually represent lower limits, since it is very unlikely that the actual MF of the disk continues to rise steeply down to  $0.1M_{\odot}$ . Moreover, this result indicates that color-shifted microlensing statistics for disk events can help distinguish between the different disk models.

The significant expected fractions of CSEs imply that many observed microlensing events will be able to provide more information than standard achromatic light curves. It is still possible that a small number of color-shifted events might already exist in the MACHO or OGLE data, but would not have been identified as such due to insufficiently precise measurement of the light curve. However, we restate that recent calculations of microlensing towards the bulge (ZRS) show that Galactic models having a mass function with 25% or more of the mass as brown dwarfs are inconsistent with current data. If the lenses are low-mass stars then color shifting will be a real effect and the cut on achromaticity must remain weak; otherwise, it would systematically exclude analysis of precisely those events from which all relevant parameters can be disentangled. In the following Section, we outline the method for obtaining these parameters.

## 7. LIGHT-CURVE ANALYSIS

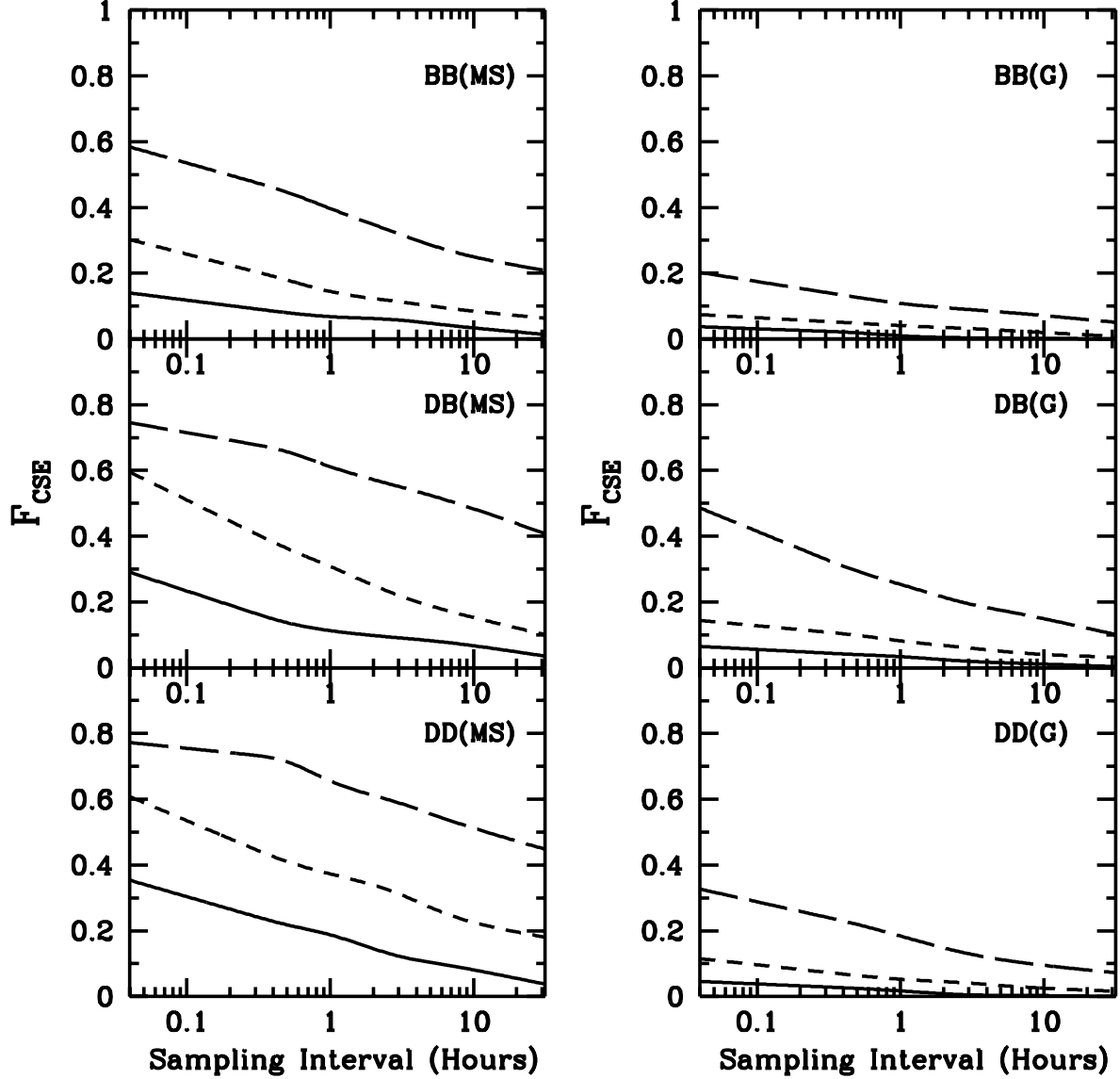


Fig. 8.— Expected  $F_{CSE}$  for events observed in  $V$  and  $I$ . The solid, short-dashed, and long-dashed lines correspond to photometric errors of 0.05, 0.01, and 0.001 mag, respectively. The various configurations are denoted by BB for bulge self-lensing, DB for disk-lensing-bulge events, and DD for disk self-lensing. MS indicates that the sources are main-sequence stars, while G indicates clump-giant sources. Accurate observations in  $V$  and  $I$  may have typical errors of several millimagnitudes and thus yield significant increases in  $F_{CSE}$ .

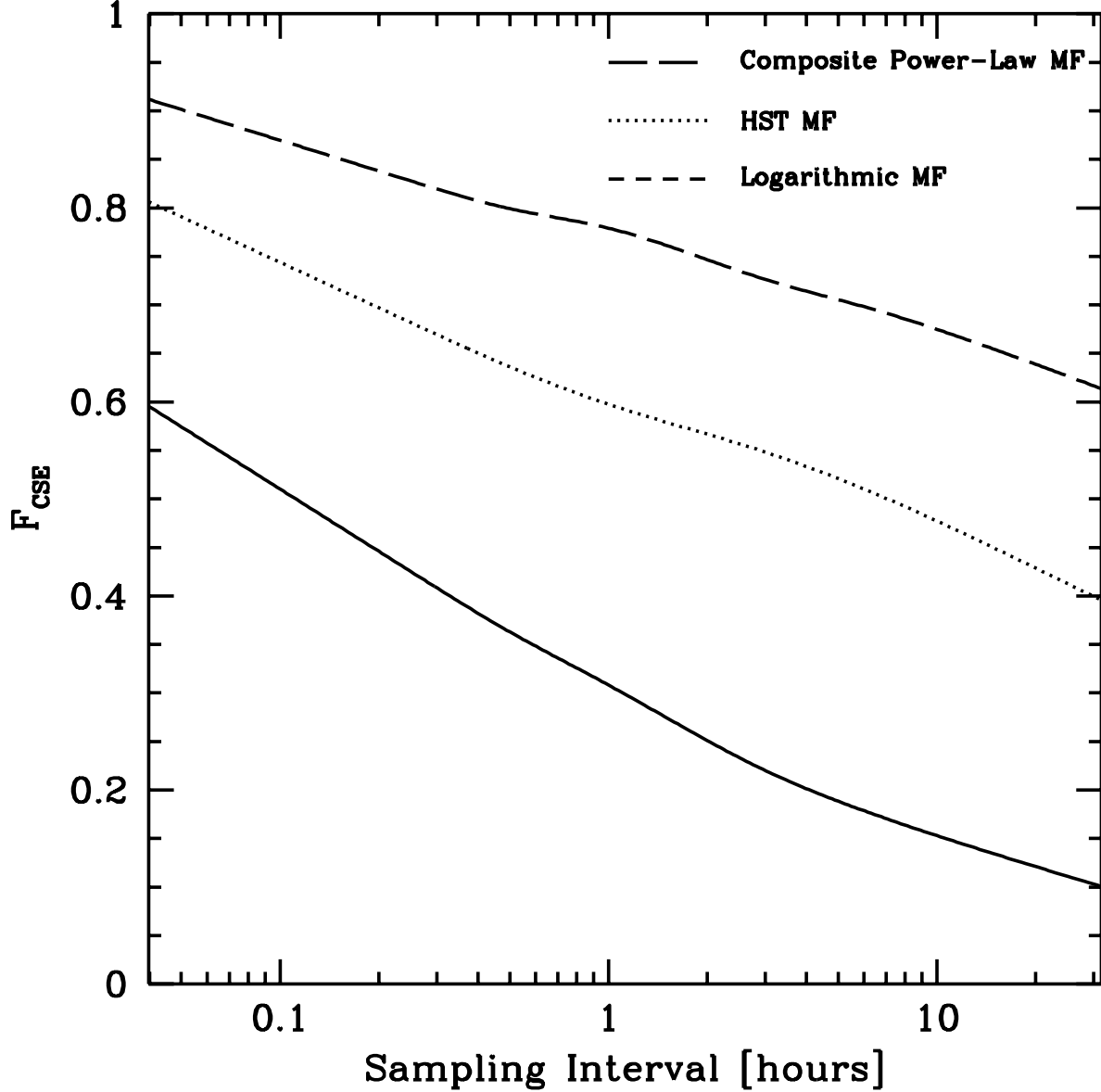


Fig. 9.—  $F_{CSE}$  vs. sampling interval for DD(MS) lensing with different disk MFs, assuming 0.01-mag errors in  $(V,I)$ . The logarithmic MF, which rises steeply to  $0.1\mathcal{M}_{\odot}$ , has the lowest median mass and predicts the fewest color-shifted events. Local observations of the disk, however, favor a MF which flattens below  $1\mathcal{M}_{\odot}$ , so the logarithmic disk MF is likely a lower limit on  $F_{CSE}$  for disk lensing.

In Section 3.1, we outlined the procedure whereby the luminosity-offset ratio in each waveband,  $r_\lambda$ , can be calculated from the masses and distances of the source and lens. Here, we follow an inverse procedure to infer the lens properties from simulated data for a “typical” microlensing event, and estimate how accurately the lens mass, distance, and transverse speed can be reconstructed from analysis of color-shifted light curves. In the following, we shall assume that observations of the source can be carried out for a sufficiently long time after the event so that the source mass and distance can be determined. We then fit measurements in two wavebands for the two unknown quantities  $\mathcal{M}_l$  and  $D_{ol}$ . Additional wavebands can be used, in principle, to make the determination more precise. For an assumed mass-luminosity relationship, Eqs. (7) and (8) can be written

$$r_{\lambda_1} = r_{\lambda_1}(\mathcal{M}_l, D_{ol}), \quad r_{\lambda_2} = r_{\lambda_2}(\mathcal{M}_l, D_{ol}). \quad (22)$$

Equations (22) can be inverted to give

$$\mathcal{M}_l = \mathcal{M}_l(r_{\lambda_1}, r_{\lambda_2}), \quad D_{ol} = D_{ol}(r_{\lambda_1}, r_{\lambda_2}). \quad (23)$$

For a given event observed in two bands,  $\lambda_1$  and  $\lambda_2$ , the light curve can be fit by the five parameters  $\mathbf{s} = \{A_{\max}, t_{\max}, t_0, r_{\lambda_1}, r_{\lambda_2}\}$ . The values for  $\mathcal{M}_l$  and  $D_{ol}$  are by obtained using Eqs. (23) with the best-fit values for  $r_{\lambda_1}$  and  $r_{\lambda_2}$ . We find that the covariance matrix for a typical CSE indicates that the errors in the  $r_\lambda$  are typically much larger than the errors in  $A_{\max}$ ,  $t_{\max}$ , and  $t_0$ . Thus, to a good approximation, the errors on  $\mathcal{M}_l$  and  $D_{ol}$  are given by

$$(\Delta\mathcal{M}_l)^2 = \left(\frac{\partial\mathcal{M}_l}{\partial r_{\lambda_1}}\right)^2 (\Delta r_{\lambda_1})^2 + \left(\frac{\partial\mathcal{M}_l}{\partial r_{\lambda_2}}\right)^2 (\Delta r_{\lambda_2})^2 \quad (24)$$

and

$$(\Delta D_{ol})^2 = \left(\frac{\partial D_{ol}}{\partial r_{\lambda_1}}\right)^2 (\Delta r_{\lambda_1})^2 + \left(\frac{\partial D_{ol}}{\partial r_{\lambda_2}}\right)^2 (\Delta r_{\lambda_2})^2. \quad (25)$$

The transverse speed can be written as  $v = R_e/t_0$ , so that the error in transverse speed becomes

$$(\Delta v)^2 = \left(\frac{dv}{dR_e}\right)^2 (\Delta R_e)^2 + \left(\frac{dv}{dt_0}\right)^2 (\Delta t_0)^2 \cong \frac{(\Delta R_e)^2}{t_0^2} \quad (26)$$

where  $(\Delta R_e)^2$  can be written explicitly in terms of  $\Delta\mathcal{M}_l$  and  $\Delta D_{ol}$  via Eq. (2), and again we neglect  $\Delta t_0$ , compared to the larger errors.

We simulate the light curve of a microlensing event, in which a  $1\mathcal{M}_\odot$  main- sequence star at 8 kpc is lensed by a  $0.4\mathcal{M}_\odot$  star at 6.25 kpc (i.e., the near end of the bulge). We assume  $t_0 = 15$  days and  $u_{\min} = 0.1$  and that the light curve is sampled every half hour in  $(V,I)$  with typical errors of 0.005 mag. Our fitting routine recovers the input parameters

with standard errors of  $\Delta\mathcal{M}_l = \pm 0.09\mathcal{M}_\odot$ ,  $\Delta D_{ol} = \pm 1.5$  kpc, and  $\Delta v = \pm 41$  km s<sup>-1</sup> at the 95% confidence level. For a similar event with  $t_0 = 40$  days, the errors become  $\Delta\mathcal{M}_l = \pm 0.05\mathcal{M}_\odot$ ,  $\Delta D_{ol} = \pm 0.95$  kpc, and  $\Delta v = \pm 25$  km s<sup>-1</sup>. The errors in the derived lens properties scale roughly linearly with the typical photometric errors for the light curve. It should be noted that since many of the events which exhibit a color shift are likely to be of relatively long duration, they may also exhibit a measurable parallax effect due to the Earth’s orbital motion (Buchalter & Kamionkowski 1995). In principle, *every* microlensing light curve is altered by this effect, but the small distortion can presently be discerned only for the longest-duration events (Alcock et al. 1995b). With the errors and sampling rates discussed above, the parallax effect could be measured for shorter-duration events and thus provide a further independent constraint on the lens transverse speed. These results show that the aforementioned intensive monitoring programs, designed to discover extra-solar planets, are ideally suited for measuring the color-shift effect as well as picking out the parallax effect to far greater accuracy than current ground-based work. The data from such surveys can remove entirely the degeneracy among the unknown lens parameters, not only for the cases where an orbiting planet is detected, but in a large fraction of events in general.

## 8. DISTINGUISHING FROM BLENDED EVENTS

Some source stars will have unresolved binary companions whose light will be blended with that of the source during the event. The effect of such blending produces a shape distortion entirely analogous to a color shift (Griest & Hu 1992). For reasonable models of the density distribution and MF of stars along the line of sight to Baade’s Window, it is intuitively evident that the majority of blends will be due to faint stars in the bulge. Thus, consider the case where the lens emits absolutely no light, but the source star is in a binary. In this case, the companion of the source star is unresolved, and light from the companion of the source star will cause shape distortions to the light curves similar to those from the case where the lens emits light. Therefore, one may question whether color shifts, if observed, signal that the lens is a luminous star. Fortunately, there are several ways of discriminating between the two scenarios. The first may be performed for each individual event. As discussed in Section 7, light-curve analysis can potentially yield the distance and mass of the star—either the lens or the unseen companion of the source star—contributing the blended light. If the distance can be determined to be different from the distance to the source star, then the blended light is most likely coming from the lens and not a binary companion to the source. One also expects that in any given event, the inferred

lens mass will in general be less than the mass of the source. If these quantities cannot be disentangled, then one cannot discriminate between the two scenarios, based on the light curve alone. High resolution imaging of stars along the line of sight, however, could likely eliminate many optical superpositions.

There is also a statistical test which can be applied to an ensemble of color-shifted events. If the lenses are emitting the blended light, then we expect the fraction of events of a given duration which are color shifted to be larger for longer-duration events. This is simply because the typical duration of an event increases for larger lens masses, and the luminosity of a dwarf increases rapidly with mass. If the lenses emit no light and the color shifts are due to blended light from a companion star, then there should be no correlation between the event duration and the color shift. Thus, in this case, the fraction of events which are color shifted should not increase as dramatically. (There will be some increase in the color-shifted fraction for longer events just because the light curve in a longer event is better sampled.) This analysis thus provides a fundamental test of whether the lenses are, in fact, ordinary stars.

To illustrate, we show in Figure 10 the expected fraction of events of a given duration whose light curves are distorted due to both of the scenarios discussed above. For color shifts from a luminous lens, we consider both bulge self-lensing (short-dashed curves) and disk-lensing-bulge events (long-dashed curves), where all stars are assumed to lie on the main sequence and follow the logarithmic mass function discussed in Section 3.2. To generate the corresponding dotted curves, we make the same assumptions about the lens and source mass and spatial distributions. However, in this case, we assume that the lens emits no light and that the color shift is due to blended light from an unresolved binary companion to the source star which has a similar mass function. In the upper panel we assume hourly sampling and 0.01-mag errors, and in the lower panel we assume 0.5 hour sampling with 0.005-mag errors, both using  $(V, I)$ . As this simple example illustrates, for BB events with  $t_0 \geq 10$  days and DB events with  $t_0 \geq 13$  days, the fraction of events which are color shifted rises more dramatically with duration if the lenses are emitting the blended light. Not all source stars are in binaries, so dot-dashed curves should actually be viewed as an upper limit to the fraction of events which are color shifted due to light from an unresolved binary. The Figure also demonstrates our previous claim that color-shift analysis is particularly important for large  $t_0$ .

## 9. CONCLUSION

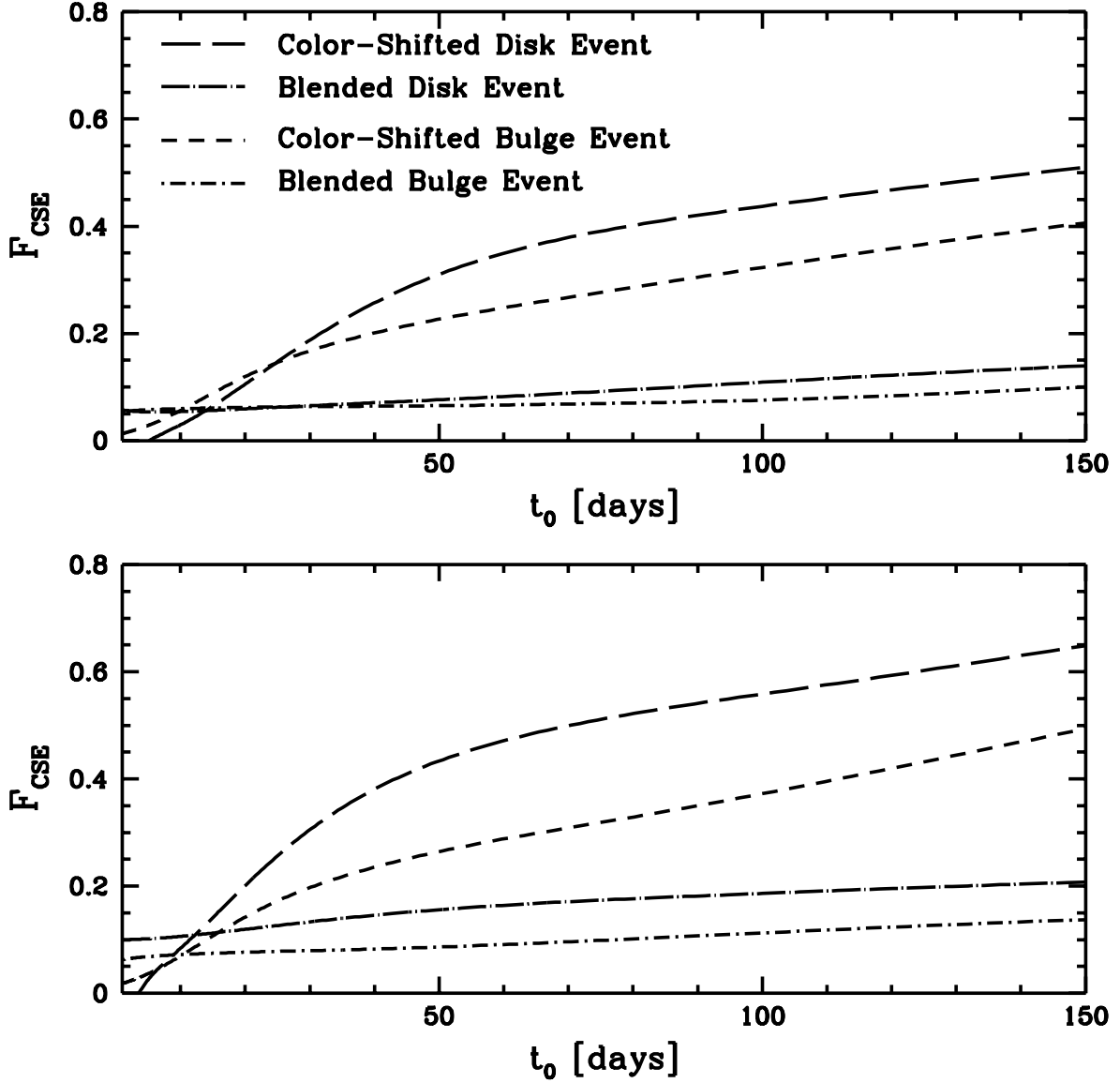


Fig. 10.— Fraction of shape-distorted events seen in  $(V,I)$  as a function of  $t_0$ . For the long-dashed and short-dashed curves,  $F_{CSE}$  arises from color shifting by the lens in DD(MS) and DB(MS) events. The dotted curves correspond to the same events, but with a dark lens and  $F_{CSE}$  arising from the blended light of a source companion. The upper panel represents hourly sampling and 0.01-mag errors while the lower panel corresponds to 0.5-hour sampling and 0.005-mag errors. The graphs show that optical blending can be ruled out statistically, and further illustrate a method to test the assumption that the lenses are stars.

The importance of microlensing surveys in the study of Galactic structure has been firmly established. The increasing wealth of data on events towards the Galactic bulge makes it increasingly unlikely that the lenses are mostly in the form of brown dwarfs and seems to indicate that they are in the form of ordinary low-mass stars. If this is the case, they are expected to give rise to a characteristic waveband-dependent shape distortion to the light curve, which can potentially be distinguished from events where the source is an optical blend. Failing to account for color shifting can lead to errors in the inferred timescales for single events and in the overall duration distribution, particularly for large  $t_0$  (Buchalter & Kamionkowski 1995). Color-shift analysis can be used with existing data to place upper limits to the lens mass as a function of distance for individual events. Our detailed calculation shows that with frequent and precise observations of events in progress, 5% to 60% of all events arising from various lens-source pairings are expected to exhibit a color shift, as observed in  $(B,K)$  or  $(V,I)$ . These events can be used to de-convolve the parameters of interest (namely  $\mathcal{M}_l$ ,  $D_{ol}$ , and  $v$ ) with reasonable precision. Moreover, it is expected that many CSEs will also exhibit a measurable parallax shift from such ground-based observations, which allows a further independent calculation of the lens characteristics. The observational requirements for measuring these effects match those of proposed planetary searches. Such surveys could thus yield important information for the study of Galactic structure, by determining important characteristics of the lensing population.

We wish to thank H. S. Zhao for providing us with data from his self-consistent model of the Galactic bar, and for helpful discussions. We also thank R. Olling for many insightful suggestions on constructing a reasonable model for the Galactic disk as well as numerous helpful comments on a preliminary draft. This work was supported in part by the U. S. Department of Energy under contract DE-FG02-92ER40699, and by NASA grants NAGW-2479 and NAG5-3091.

## REFERENCES

- Alard, C. et al. 1995, *Msngr*, 80, 31
- Alcock, C. et al. 1993, *Nature*, 365, 621
- Alcock, C. et al. 1994, *BAAS*, 185, #17.03
- Alcock, C. et al. 1995a, *ApJ*, 445, 133
- Alcock, C. et al. 1995b, *astro-ph/9506114*

- Allen, C. W. 1973, *Astrophysical Quantities* (London: The Athelone Press)
- Arp, H. 1965, *ApJ*, 141, 43
- Aubourg, E. et al. 1993, *Nature*, 365, 623
- Bennett, D. P. et al. 1995, astro-ph/941114
- Binney J. et al. 1991, *MNRAS*, 252, 210
- Blitz, L. & Spergel D. N. 1991, *ApJ*, 379, 631
- Buchalter, A. & Kamionkowski, M. 1995, in preparation
- Caldwell, J. et al. 1993, *SAAO Circulars*, no. 15
- Cook, K. et al. 1994, *BAAS*, 185, #17.04
- Dwek, E. et al. 1995, *ApJ*, 445, 716
- Giudice, G. F., Mollerach, S., & Roulet, E. 1994, *Phys. Rev. D*, 50, 2406
- Gould, A., Bahcall, J. N., & Flynn, C. 1995, astro-ph/9505087
- Gould, A. 1994a, astro-ph/9408060
- Gould, A. 1994b, OSU-TA-15/94, astro-ph/9408032, *ApJ*, submitted
- Gould, A. 1995a, *ApJ*, 441, L21
- Gould, A. 1995b, *ApJ*, 440, 510
- Gould, A. & Loeb, A 1992, *ApJ*, 104,114
- Griest, K. 1991, *ApJ*, 366, 412
- Griest, K. et al. 1991, *ApJ*, 372, L79
- Griest, K. & Hu, W. 1992, *ApJ*, 397, 362
- Griest, K. 1995, private communication
- Han, C. & Gould, A. 1995a, *ApJ*, 447, 53
- Han, C. & Gould, A. 1995b, astro-ph/9504078
- Henry, T. J. & McCarthy, W. 1993, *AJ*, 106, 773
- Jungman, G., Kamionkowski, M., Kosowsky, A., & Spergel, D. N. 1995, astro-ph/9507080, *Phys. Rev. Lett.*, in press
- Kamionkowski, M. 1995, *ApJ*, 442, L9
- Kamionkowski, M. & Buchalter, A. 1995, Talk given (by MK) at Microlensing Workshop, January 13-15, 1995, Livermore, CA
- Kiraga, M. & Paczyński, B. 1994, *ApJ*, 430, L101 (KP)

- Larson, R. 1986, MNRAS, 256, 641
- Lewis, J. R. & Freeman, K. C. 1989, AJ, 97, 139
- Loeb, A. & Sasselov, D. 1995, ApJ, 449, L33
- Maoz, D. & Gould, A. 1994, ApJ, 425, L67
- Merrifield, M. R. 1992, AJ, 103, 1552
- Mihalas, D. & Binney, J. 1982, Galactic Astronomy (New York: Freeman)
- Mollerach, S. & Roulet, E. 1995, astro-ph/9510063
- Nemiroff, R. J. & Wickramasinghe, W. A. D. T. 1994, ApJ, 424, L21
- Paczyński, B. et al. 1994, AJ, 107, 2060
- Paczyński, B. 1986, ApJ, 304, 1
- Rich, R. M. 1988, AJ, 95, 828
- Rich, R. M. 1990, ApJ, 362, 604
- Rodgers, A. W. & Harding, P. 1989, ApJ 97, 1036
- Savage, B. D. & Mathis, J. S. 1979, ARA&A, 17, 73
- Scalo, J. M. 1986, Fundamentals of Cosmic Physics (New York: Gordon & Breach)
- Spaenhauer, A., Jones, B. F., & Whitford, A. E. 1992, AJ, 103, 297
- Stanek K. Z. et al. 1994, ApJ, 429, L73
- Stubbs, C. et al. 1994, BAAS, 185, #17.07
- Tytler, D. et al. 1996, in preparation
- Udalski, A. et al. 1994a, AcA, 44, 165
- Udalski, A. et al. 1994b, AcA, 44, 227
- Udalski, A. et al. 1994c, astro-ph/9407084, to appear in ApJ
- Vandenberg, D. A. & Laskarides, P. G. 1987, ApJS, 64, 103
- van der Kruit, P. C. 1990, The Milky Way as a Galaxy (Mill Valley: University Science Books)
- van der Kruit, P. C. 1988, A&A, 221, 236
- Whitelock P. & Catchpole R. 1992, in The Center, Bulge and Disk of the Milky Way, ed. L. Blitz (Dordrecht: Kluwer), 103
- Zhao, H. S. 1995, MNRAS, in press
- Zhao, H. S., Spergel, D. N., & Rich, R. M. 1995, ApJ, 440, L13 (ZSR)

Zhao, H.S., Rich R. M., & Spergel, D. N. 1995, in preparation (ZRS)